bioRxiv preprint doi: https://doi.org/10.1101/2021.08.29.458125; this version posted August 31, 2021. The copyright holder for this preprint (which was not certified by peer review) is the author/funder, who has granted bioRxiv a license to display the preprint in perpetuity. It is made available under aCC-BY 4.0 International license.

NBI-921352, a First-in-Class, $Na_V1.6$ Selective, Sodium Channel Inhibitor That Prevents Seizures in *Scn8a* Gain-of-Function Mice, and Wild-Type Mice and Rats

JP Johnson Jr[2], Thilo Focken[4], Kuldip Khakh[2], Parisa Karimi Tari[1], Celine Dube[1], Aaron Williams[2], Jean-Christophe Andrez[4], Girish Bankar[1], David Bogucki[4], Kristen Burford[4], Elaine Chang[2], Sultan Chowdhury[4], Richard Dean[2], Gina de Boer[5], Shannon Decker[4], Christoph Dehnhardt[4], Mandy Feng[2], Wei Gong[4], Samuel J Goodchild[2], Michael Grimwood[4], Abid Hasan[4], Angela Hussainkhel[2], Qi Jia[4], Stephanie Lee[5], Jenny Li[2], Sophia Lin[2], Andrea Lindgren[5], Verner Lofstrand[4], Janette Mezeyova[2], Rostam Namdari[6], Karen Nelkenbrecher[1], Noah Gregory Shuart[2], Luis Sojo[5], Shaoyi Sun[4], Matthew Taron[4], Matthew Waldbrook[1], Diana Weeratunge[2], Steven Wesolowski[4], Michael Wilson[4], Zhiwei Xie[2], Rhena Yoo[2], Clint Young[2], Alla Zenova[4], Wei Zhang[4], Alison J Cutts[3], Robin P Sherrington[7], Simon N Pimstone[7], Raymond Winquist[7], Charles J Cohen[7], James R Empfield[7]

Xenon Pharmaceuticals Inc.
In Vivo Biology[1], In Vitro Biology[2], Scientific Affairs[3], Chemistry[4], Compound Properties[5], Translational Drug Development[6], Executive Team[7]

bioRxiv preprint doi: https://doi.org/10.1101/2021.08.29.458125; this version posted August 31, 2021. The copyright holder for this preprint (which was not certified by peer review) is the author/funder, who has granted bioRxiv a license to display the preprint in perpetuity. It is made available under aCC-BY 4.0 International license.

Abstract

NBI-921352 (formerly XEN901) is a novel sodium channel inhibitor designed to specifically target $Na_V1.6$ channels. Such a molecule provides a precision-medicine approach to target *SCN8A*-related epilepsy syndromes (*SCN8A*-RES), where gain-of-function (GoF) mutations lead to excess $Na_V1.6$ sodium current, or other indications where $Na_V1.6$ mediated hyper-excitability contributes to disease (Gardella and Moller, 2019; Johannesen et al., 2019; Veeramah et al., 2012). NBI-921352 is a potent inhibitor of $Na_V1.6$ (IC_{50} 0.051 µM), with exquisite selectivity over other sodium channel isoforms (selectivity ratios of 756X for $Na_V1.1$, 134X for $Na_V1.2$, 276X for $Na_V1.7$, and >583X for $Na_V1.3$, $Na_V1.4$, and $Na_V1.5$). NBI-921352 is a state-dependent inhibitor, preferentially inhibiting activated (inactivated or open) channels. The state dependence leads to potent stabilization of inactivation, inhibiting $Na_V1.6$ currents, including resurgent and persistent $Na_V1.6$ currents, while sparing the closed/rested channels. The isoform-selective profile of NBI-921352 led to a robust inhibition of action-potential firing in glutamatergic excitatory pyramidal neurons, while sparing fast-spiking inhibitory interneurons, where $Na_V1.1$ predominates. Oral administration of NBI-921352 prevented electrically induced seizures in a *Scn8a* GoF mouse, as well as in wild-type mouse and rat seizure models. NBI-921352 was effective in preventing seizures at lower brain and plasma concentrations than commonly prescribed sodium channel inhibitor antiseizure medicines (ASMs) carbamazepine, phenytoin, and lacosamide. NBI-921352 was well tolerated at higher multiples of the effective plasma and brain concentrations than those ASMs. NBI-921352 is entering phase II proof-of-concept trials for the treatment of *SCN8A*-developmental epileptic encephalopathy (*SCN8A*-DEE) and adult focal-onset seizures.

bioRxiv preprint doi: https://doi.org/10.1101/2021.08.29.458125; this version posted August 31, 2021. The copyright holder for this preprint (which was not certified by peer review) is the author/funder, who has granted bioRxiv a license to display the preprint in perpetuity. It is made available under aCC-BY 4.0 International license.

Introduction

$Na_V1.6$ voltage-gated sodium channels are widely expressed in the brain and are important contributors to neural excitability (Meisler, 2019; Royeck et al., 2008). Mutations in the *SCN8A* gene result in malfunction of $Na_V1.6$ sodium channels and cause a spectrum of *SCN8A*-related syndromes in humans, and disruptions of mouse $Na_V1.6$ likewise disrupt normal physiology (Burgess et al., 1995; Gardella and Moller, 2019; Johannesen et al., 2019; Meisler, 2019; Veeramah et al., 2012; Wagnon et al., 2015). Variants of $Na_V1.6$ channels can result in either gain or loss of function. Loss-of-function (LoF) variants in humans are generally associated with autism spectrum disorders with cognitive and developmental delay without epilepsy (Inglis et al., 2020; Liu et al., 2019), but, in some cases, can lead to late-onset seizures. In mice, LoF variants of $Na_V1.6$ lead to motor impairment but increase seizure resistance (Hawkins et al., 2011; Martin et al., 2007). Gain-of-function (GoF) variants in human *SCN8A* generally result in early-onset *SCN8A*-related epilepsy syndromes (*SCN8A*-RES). The most severe of these epilepsy syndromes is *SCN8A* developmental and epileptic encephalopathy (*SCN8A*-DEE) (Gardella and Moller, 2019; Hammer et al., 2016; Johannesen et al., 2019). Most *SCN8A*-RES patients carry de novo heterozygous missense variants that lead to a gain of function of the $Na_V1.6$ channel, though inherited and bi-allelic variants have been reported (Gardella and Moller, 2019; Wengert et al., 2019). *SCN8A*-DEE patients present early in life with seizure onset usually occurring in the first year of life. After seizure onset, patients begin to miss developmental milestones and display additional symptoms, including cognitive and motor delay, hypotonia

bioRxiv preprint doi: https://doi.org/10.1101/2021.08.29.458125; this version posted August 31, 2021. The copyright holder for this preprint (which was not certified by peer review) is the author/funder, who has granted bioRxiv a license to display the preprint in perpetuity. It is made available under aCC-BY 4.0 International license.

and cortical blindness. *SCN8A*-DEE individuals are predisposed to early death, including sudden unexplained death in epilepsy (SUDEP). While *SCN8A*-RES patients often have treatment-resistant seizures, many can achieve seizure reduction or seizure freedom upon treatment with anti-seizure medicines (ASMs) that non-selectively inhibit voltage-gated sodium channels, like phenytoin (Boerma et al., 2016; Braakman et al., 2017). *SCN8A*-RES patients may require doses that are higher than those prescribed for most epilepsy patients and, as a result, can be more prone to drug-related adverse events (Boerma et al., 2016; Gardella and Moller, 2019). Even with high doses and multiple ASMs, many patients continue to have uncontrolled seizures as well as extensive comorbidities. The aggressive pharmacotherapy required to protect *SCN8A* patients from life-threatening seizures often comes with attendant side effects that would not be tolerated in less severely impacted populations.

Existing sodium channel inhibitor ASMs are nonselective, blocking all voltage-gated sodium channel isoforms at similar plasma or brain concentrations. This lack of selectivity likely limits the benefits of sodium channel inhibitors since LoF variants of $Na_V1.1$ are known to impair inhibitory interneuron function and cause generalized epilepsy with seizures plus (GEFS+) and *SCN1A*-DEE (Dravet Syndrome) (Catterall et al., 2010; Claes et al., 2001; Escayg et al., 2000; Gennaro et al., 2003). Thus, inhibiting $Na_V1.1$ may counter the benefit of inhibiting the sodium channels of excitatory neurons. Inhibiting $Na_V1.4$ and $Na_V1.5$ currents is also undesirable since those channels are critical for facilitating contraction of skeletal and cardiac muscles, respectively (Chen et al., 1998; Ptacek et al., 1991; Rojas et al., 1991).

We hypothesized that a selective inhibitor of $Na_V1.6$ could provide a safer and more effective treatment for patients with *SCN8A*-RES and might also be more broadly efficacious in more

bioRxiv preprint doi: https://doi.org/10.1101/2021.08.29.458125; this version posted August 31, 2021. The copyright holder for this preprint (which was not certified by peer review) is the author/funder, who has granted bioRxiv a license to display the preprint in perpetuity. It is made available under aCC-BY 4.0 International license.

common forms of epilepsy. An extensive medicinal-chemistry effort produced NBI-921352, the first potent and selective inhibitor of $Na_V1.6$ channels (Neurocrine, 2019). We explored the profile of NBI-921352 in vitro, ex vivo and in three preclinical in vivo rodent seizure models, including electrically induced seizure assays in genetically engineered mice bearing heterozygous *Scn8a* GoF $Na_V1.6$ channels (N1768D), as well as in wild-type mice and rats.

Results

In vitro Na_V potency and selectivity

Human Na_V channel isoforms $hNa_V1.1$, $hNa_V1.2$, $hNa_V1.3$, $hNa_V1.4$, $hNa_V1.5$, $hNa_V1.6$, and $hNa_V1.7$ were heterologously expressed in HEK-293 cells, and the potency and isoform selectivity of NBI-921352 (Figure 1, Table 1) was determined by automated patch-clamp techniques. NBI-921352 potently inhibited $hNa_V1.6$ channel currents with an inhibitory concentration 50% (IC_{50}) of 0.051 µM (95% CI: 0.030 to 0.073 µM; N=3) calculated from 3 biological replicates. Inhibition of other human $Na_V1.X$ isoforms required higher concentrations of NBI-921352 with IC_{50}'s of 39 µM (95% CI: 31 to 47 µM; N=3) for $hNa_V1.1$, 6.9 µM (95% CI: 1.6 to 12 µM; N=3) for $hNa_V1.2$, >30 µM for $hNa_V1.3$, >30 µM for $hNa_V1.4$, >30 µM for $hNa_V1.5$, and 14 µM (95% CI: 6.4 to 22 µM; N=3) for $hNa_V1.7$. These potencies provide selectivity ratios for $hNa_V1.6$ versus the other hNa_V isoforms (IC_{50} $hNa_V1.X$ / IC_{50} $hNa_V1.6$) of 756 ($Na_V1.1$), 134 ($Na_V1.2$), 276 ($Na_V1.7$) and >583 ($Na_V1.3$, $Na_V1.4$, $Na_V1.5$).

Since we intended to evaluate in vivo effects of NBI-921352 in mouse seizure models, we also assessed the potency of NBI-921352 in the mouse Na_V isoforms that are most highly expressed in the brain, $Na_V1.6$, $Na_V1.1$, and $Na_V1.2$. The potency and selectivity in mouse Na_V channels

bioRxiv preprint doi: https://doi.org/10.1101/2021.08.29.458125; this version posted August 31, 2021. The copyright holder for this preprint (which was not certified by peer review) is the author/funder, who has granted bioRxiv a license to display the preprint in perpetuity. It is made available under aCC-BY 4.0 International license.

closely paralleled that seen in the human orthologues with IC_{50}'s of 0.058 µM (95% CI: 0.046 to 0.070 µM; N=3) for mNa$_V$1.6, 41 µM (95% CI: 30 to 52 µM; N=3) for mNa$_V$1.1, and 11 µM (95% CI: 8.2 to 14 µM; N=3) for mNa$_V$1.2. Selectivity ratios (IC_{50} mNa$_V$1.X / IC_{50} mNa$_V$1.6) were 709 (Na$_V$1.1), and 191 (Na$_V$1.2). These data indicate that NBI-921352 potently inhibits both human and mouse Na$_V$1.6 channels, and that it does so at concentrations ≥ 134-fold lower than for any of the other channel isoforms tested.

NBI-921352 inhibited patient-identified variants of Na$_V$1.6 channels

Patients with *SCN8A*-RES carry missense variants in the Na$_V$1.6 channel. A great number of variants have been identified, with a range of biophysical defects. Since most variants are de novo, many have been identified in only one or a few patients. For this reason, we determined the effectiveness of NBI-921352 to inhibit 9 patient identified variants spread across the channel (Figure 2, Table 2) (Gardella and Moller, 2019; Wagnon and Meisler, 2015). The 9 variants studied have all been identified in *SCN8A*-RES patients and are in Domains II, III, and IV. Inhibition of the mutant channel constructs was evaluated by automated patch-clamp electrophysiological techniques after transient transfection of the human Na$_V$1.6 variant construct of interest into Expi293F™ cells. All the variants were sensitive to inhibition by NBI-921352. Observed IC_{50}s for inhibition were 0.051 µM (WT mean from Figure 1), 0.031 µM (95% CI: 0.027 to 0.037 µM) (T767I), 0.021 µM (95% CI: 0.017 to 0.026 µM) (R850Q), 0.032 µM (95% CI: 0.029 to 0.036 µM) (N984K), 0.035 µM (95% CI: 0.029 to 0.043 µM) (I1327V), 0.039 µM (95% CI: 0.031 to 0.050 µM) (N1466K), 0.34 µM (95% CI: 0.26 to 0.44 µM) (R1617Q), 0.055 µM (95% CI: 0.046 to 0.064 µM) (N1768D), 0.068 µM (95% CI: 0.054 to 0.085 µM) (R1872W), and 0.035 µM (95% CI: 0.029 to 0.041 µM) (N1877S). We found that 8 of the 9 variants were inhibited

bioRxiv preprint doi: https://doi.org/10.1101/2021.08.29.458125; this version posted August 31, 2021. The copyright holder for this preprint (which was not certified by peer review) is the author/funder, who has granted bioRxiv a license to display the preprint in perpetuity. It is made available under aCC-BY 4.0 International license.

with a potency similar to that of the wild-type channel, with most being slightly more potently inhibited. Only one variant, N1617Q, required markedly higher concentrations of NBI-921352 for inhibition, with an IC_{50} for inhibition 6.6-fold higher than that of the wild-type $Na_V1.6$ channel. The reduced potency for N1617Q is consistent with the variant residing in the predicted binding site of NBI-921352 in the domain IV voltage sensor, see discussion.

NBI-921352 is a state-dependent inhibitor

Many small molecule inhibitors of Na_V channels bind preferentially to open and or inactivated states (Bean et al., 1983; Courtney et al., 1978; Strichartz, 1976). To query the state dependence of NBI-921352, we measured the apparent potency with two different voltage protocols that favor either the closed (rested) state or activated (open and inactivated) states (Figure 3). Holding the membrane potential at -120 mV induces most channels to reside in the resting state. Brief depolarizations to measure $Na_V1.6$ current enabled the determination of an IC_{50} of 36 µM (95% CI: 29 to 47 µM) for rested-state channels. Holding the membrane potential at -45 mV encourages channels to transition into open and inactivated states. Brief hyperpolarizations allow rapid recovery from inactivation for channels that are not bound to drug followed by a short 20 ms test pulse to -20 mV to measure currents from unbound channels (see methods for details). Measuring the ability of NBI-921352 to inhibit reopening of activated channels leads to an apparent IC_{50} of 0.051 µM (Figures 1 and 3). Thus, NBI-921352 strongly prefers activated (open or inactivated) channels, inhibiting them at concentrations more than 750-fold less than those needed to inhibit rested or “peak” sodium currents.

bioRxiv preprint doi: https://doi.org/10.1101/2021.08.29.458125; this version posted August 31, 2021. The copyright holder for this preprint (which was not certified by peer review) is the author/funder, who has granted bioRxiv a license to display the preprint in perpetuity. It is made available under aCC-BY 4.0 International license.

NBI-921352 inhibited persistent and resurgent currents from mutant $Na_V1.6$ channels

The state-dependent nature of inhibition is also revealed in other types of voltage-clamp protocols, including those designed to measure persistent or resurgent sodium currents. Some drugs or candidate drugs, like PRAX-330 and Riluzole, have been touted based on their preference for persistent currents, but, in fact, this is a feature of all the compounds in Na_V inhibitor class. Apparent differences in persistent current selectivity are driven by differential kinetics and concentration dependences in combination with the electrophysiological protocols chosen for the measurements.

Elevated persistent and or resurgent currents are believed to underlie or contribute to the pathology of many sodium channel related pathologies (Mason et al., 2019; Pan and Cummins, 2020; Potet et al., 2020; Tidball et al., 2020; Zaman et al., 2019). In most conditions, normal $Na_V1.6$ channels inactivate rapidly and nearly completely after opening. Persistent currents result from channels that are not stably inactivated – a common phenotype for epilepsy-inducing variants in $Na_V1.6$, including N1768D (Tidball et al., 2020; Wagnon et al., 2015). We found that NBI-921352 inhibited N1768D $Na_V1.6$ persistent currents (measured as the non-inactivating current 10 ms after initiation of the depolarizing test pulse) with a similar potency as for open and inactivated wild-type $Na_V1.6$ channels with an IC_{50} of 0.059 µM (95% CI: 0.044 to 0.082 µM) (Figure 3).

Resurgent currents occur after repolarizing following a strong depolarization as channels redistribute between closed, open, and inactivated states (Raman and Bean, 1997). These resurgent currents are enhanced in many *SCN8A*-RES variants (Pan and Cummins, 2020; Raman

bioRxiv preprint doi: https://doi.org/10.1101/2021.08.29.458125; this version posted August 31, 2021. The copyright holder for this preprint (which was not certified by peer review) is the author/funder, who has granted bioRxiv a license to display the preprint in perpetuity. It is made available under aCC-BY 4.0 International license.

et al., 1997). NBI-921352 also effectively inhibited resurgent currents from N1768D channels with apparent IC_{50} of 0.037 µM (95% CI: 0.025 to 0.060 µM).

NBI-921352 preferentially inhibited excitatory pyramidal neurons and spared inhibitory interneurons.

A primary goal of creating $Na_V1.6$ selective inhibitors was to spare $Na_V1.1$, the voltage-gated sodium channel that is most prevalent in inhibitory interneurons. This should allow the selective targeting of excitatory neurons, where $Na_V1.6$ and $Na_V1.2$ are believed to be dominant, over inhibitory interneurons. To test this hypothesis, we performed current-clamp experiments in glutamatergic pyramidal neurons from mouse layer 5 neocortex and from fast spiking interneurons in the same region. Application of 0.250 µM NBI-921352 decreased the maximum firing rate in all pyramidal neurons tested (Figure 4A). This reduction was significantly different from control values at current injection intensities between 120 pA and 320 pA ($n = 3$, $p<0.05$, paired 2-tailed student's t-test), except for 310 pA ($p = 0.051$). In contrast, NBI-921352 subtly increased the number of action potentials (APs) in fast-spiking inhibitory interneurons (Figure 4B) in a statistically significant manner at multiple current injection levels (see Figure 4B). In contrast, carbamazepine inhibited action-potential firing in both pyramidal neurons and in fast-spiking interneurons to a similar degree. The Figure 4 insets show the paired effects of compound on AP number from a stimulus injection of approximately 3X the control Rheobase for that neuron (Pyramidal NBI-921352: 200 pA, Pyramidal carbamazepine: 160 pA, Interneuron NBI-921352: 220 pA, Interneuron carbamazepine: 300 pA).

bioRxiv preprint doi: https://doi.org/10.1101/2021.08.29.458125; this version posted August 31, 2021. The copyright holder for this preprint (which was not certified by peer review) is the author/funder, who has granted bioRxiv a license to display the preprint in perpetuity. It is made available under aCC-BY 4.0 International license.

NBI-921352 inhibited electrically induced seizures in *Scn8a*$^{N1768D/+}$ mice

A selective inhibitor of $Na_V1.6$ should lend itself to the treatment of disease states caused by pathologic gain of function of $Na_V1.6$ channels. Hence, we examined the ability of NBI-921352 to inhibit electrically induced seizures in mice with a patient-identified GoF variant in the *Scn8a* gene encoding $Na_V1.6$. N1768D is a variant of $Na_V1.6$ identified in the first reported *SCN8A*-DEE patient (Veeramah et al., 2012). N1768D $Na_V1.6$ channels have impaired voltage-dependent inactivation gating that results in persistent sodium currents and enhanced resurgent currents. Because $Na_V1.6$ channels are highly expressed in the neurons of the brain, increased sodium flux in excitatory neurons leads to seizures. Genetically modified mice bearing the same variant (*Scn8a*$^{N1768D/+}$) were created and found to be seizure prone, producing a mouse model with a similar phenotype as that observed in *SCN8A*-DEE patients (Wagnon et al., 2015). Some *Scn8a*$^{N1768D/+}$ mice develop spontaneous seizures at age p60 to p100, but seizure onset and frequency is quite variable, making spontaneous seizure studies challenging. In addition, mice rapidly clear NBI-921352, making it extremely difficult to maintain drug plasma and brain levels in an efficacious range for chronic or subchronic dosing experiments. As an alternative means of assessing NBI-921352's ability to engage $Na_V1.6$ channels in vivo, we designed a modified version of the 6Hz psychomotor seizure assay in *Scn8a*$^{N1768D/+}$ mice (Barton et al., 2001; Focken et al., 2019). A mild current stimulation (12 mA) evoked robust generalized tonic-clonic seizures (GTC) with hindlimb extension in *Scn8a*$^{N1768D/+}$ mice, but not in wild-type littermates.

Oral administration of NBI-921352 two hours prior to electrical stimulation prevented induction of GTC with hindlimb extension in *Scn8a*$^{N1768D/+}$ mice in a dose-dependent manner with a 50% effective dose (ED_{50}) of 15 mg/kg (95% CI 9.6 to 23 mg/kg, see Figure 5A).

bioRxiv preprint doi: https://doi.org/10.1101/2021.08.29.458125; this version posted August 31, 2021. The copyright holder for this preprint (which was not certified by peer review) is the author/funder, who has granted bioRxiv a license to display the preprint in perpetuity. It is made available under aCC-BY 4.0 International license.

After seizure assessment, all animals were euthanized, and the concentration of NBI-921352 was determined in the plasma and brain tissue from each mouse. The average concentrations for each dose group were used to generate plasma concentration and brain concentration versus efficacy relationships (Figures 5B and 5C, respectively). The plasma 50% effective concentration (EC_{50}) was 0.037 µM (95% CI 0.018 to 0.090 µM, see Figure 5B). The brain EC_{50} was 0.064 µM (95% CI 0.045 to 0.091 µM, see Figure 5C).

NBI-921352 inhibited electrically induced seizures in wild-type mice

$Na_V1.6$ is an important mediator of neuronal excitability even in animals without GoF mutations. For this reason, we wondered whether NBI-921352 might have broader application in epilepsy beyond *SCN8A*-RES and in other syndromes of neural hyperexcitability. To gain insight into this possibility, we assessed NBI-921352 in a MES assay induced by direct-current electrical stimulus (DC-MES, see methods) in wild-type mice. Figures 5D, E & F show that NBI-921352 prevented GTC with hindlimb extension induction in the DC-MES assay in a dose- and concentration-dependent manner. The ED_{50} for NBI-921352 was 23 mg/kg (95% CI 16 to 34 mg/kg, see Figure 5D). The efficacy of NBI-921352 was also concentration dependent with a plasma EC_{50} of 0.52 µM (95% CI 0.25 to 1.2 µM, see Figure 5E) and a brain EC_{50} of 0.20 µM (95% CI 0.12 to 0.38 µM, see Figure 5F).

NBI-921352 inhibited electrically induced seizures in wild-type rats

To further explore the preclinical efficacy of NBI-921352, we assessed NBI-921352 in a MES assay induced by direct-current electrical stimulus in wild-type Sprague Dawley rats (see methods). Figures 5G, H & I show that NBI-921352 prevented GTC with hindlimb-extension

bioRxiv preprint doi: https://doi.org/10.1101/2021.08.29.458125; this version posted August 31, 2021. The copyright holder for this preprint (which was not certified by peer review) is the author/funder, who has granted bioRxiv a license to display the preprint in perpetuity. It is made available under aCC-BY 4.0 International license.

induction in the rat DC-MES assay in a dose- and concentration-dependent manner. The ED_{50} for NBI-921352 was 3.7 mg/kg (95% CI 2.3 to 7.6 mg/kg, see Figure 5G). The efficacy of NBI-921352 was also concentration dependent with a plasma EC_{50} of 0.15 µM (95% CI 0.09 to 0.31 µM, see Figure 5H) and a brain EC_{50} of 0.037 µM (95% CI 0.028 to 0.054 µM, see Figure 5I).

Repeated-dosing efficacy in mice and rats

We found that repeated dosing tended to increase efficacy at lower doses and exposures of NBI-921352 than after a single dose (Figure 5, red symbols). Animals were dosed every 12 hours, morning, and evening for 13 doses. Two hours after the 13th dose, on the seventh day, efficacy was tested as in acute-dosing studies. A trend toward improved efficacy was noted in all three assays (see red symbols in Figure 5), but the improvement was not statistically significant when comparing single-dose groups to repeated-dose groups at the same dose level in the same experiment. NBI-921352 did not appreciably accumulate in the plasma or tissue and therefore any trends in improved efficacy were not explained by higher drug concentrations.

NBI-921352 is effective at lower brain concentrations than three Na_V inhibitor ASMs

Both the efficacy and adverse events of Na_V inhibitors is driven by the drugs action in the central nervous system (CNS). We found that NBI-921352 was effective in the three preclinical seizure models evaluated at markedly lower brain concentrations than carbamazepine, phenytoin, and lacosamide (Figure 6). The brain EC_{50}s for carbamazepine were 9.4 µM, 44 µM, and 36 µM for the *Scn8a*$^{N1768D/+}$ 6Hz model, WT mouse DC-MES, and WT rat DC-MES models, respectively. The brain EC_{50}s for phenytoin were 18 µM, 13 µM, and 2.6 µM for the *Scn8a*$^{N1768D/+}$ 6Hz model, WT mouse DC-MES, and WT rat DC-MES models, respectively. The

bioRxiv preprint doi: https://doi.org/10.1101/2021.08.29.458125; this version posted August 31, 2021. The copyright holder for this preprint (which was not certified by peer review) is the author/funder, who has granted bioRxiv a license to display the preprint in perpetuity. It is made available under aCC-BY 4.0 International license.

brain EC_{50}s for lacosamide were 3.3 µM, 7.1 µM, and 4.3 µM for the *Scn8a*$^{N1768D/+}$ 6Hz model, WT mouse DC-MES, and WT rat DC-MES models, respectively. The lower brain concentrations required for efficacy with NBI-921352 are consistent with the potent inhibition of $Na_V1.6$ produced by NBI-921352 (Figure 1).

NBI-921352 provided improved separation between efficacy in rats and behavioral signs

The intent of creating a highly selective $Na_V1.6$ antagonist was to reproduce or improve on the efficacy of classic, nonselective, sodium channel inhibitor drugs while reducing or preventing the adverse events caused by polypharmacy with other sodium channel and non-sodium channel targets. If sparing $Na_V1.1$ and other off-target interactions does, in fact, reduce adverse events, then even higher receptor occupancy of $Na_V1.6$ might be achievable, thereby further improving efficacy.

To evaluate our hypothesis, we compared the window between the plasma concentrations required for efficacy (plasma EC_{50}) relative to the minimal plasma concentration at which treated rats showed behavioral signs of adverse effects as reported by the blinded experimenter (Figure 7). We made this comparison both for NBI-921352 and for several widely used Na_V inhibitor ASMs: carbamazepine, phenytoin, and lacosamide.

NBI-921352 was well tolerated in these studies up to a plasma concentration of 71 µM. Dividing this concentration by the plasma EC_{50} of 0.15 µM in the rat DC-MES study results in a behavioral signs concentration (BSC) / plasma EC_{50} ratio of 473-fold. The same calculation was repeated for the established ASMs. The minimal plasma concentrations provoking behavioral signs for carbamazepine, phenytoin, and lacosamide were 110 µM, 11 µM, and 123 µM,

bioRxiv preprint doi: https://doi.org/10.1101/2021.08.29.458125; this version posted August 31, 2021. The copyright holder for this preprint (which was not certified by peer review) is the author/funder, who has granted bioRxiv a license to display the preprint in perpetuity. It is made available under aCC-BY 4.0 International license.

276 respectively. Their plasma EC_{50}s were 30 µM, 4.5 µM, and 24.4 µM, respectively. Figure 7E
277 shows BSC / Plasma EC_{50} ratios for carbamazepine (3.7-fold), phenytoin (2.4-fold), and
278 lacosamide (5.0-fold). This data indicates that increasing $Na_V1.6$ selectivity can improve the
279 tolerability of Na_V inhibitors in rodent-seizure models.

280

281 Discussion

282 Sodium channel inhibitors have long been, and remain, a mainstay of pharmacotherapy for
283 epilepsy, as well as for pain and other neurologic, cardiac, and skeletal muscle disorders. The
284 diverse range of indications and systems affected by these drugs is a testament to their critical
285 biological role in cellular excitability. A fundamental challenge for these currently marketed
286 sodium channel drugs is that none of them are selective amongst the nine sodium channel
287 isoforms. As a result, drugs targeting the sodium channels of the brain for epilepsy can inhibit
288 both excitatory and inhibitory neurons, limiting their ability to restore balanced neuronal firing.

289 Reducing $Na_V1.1$ current is proconvulsant due to the predominance of $Na_V1.1$ in inhibitory
290 interneurons (Catterall et al., 2010; Claes et al., 2001; Escayg et al., 2000; Mistry et al., 2014; Yu
291 et al., 2006), while the opposite is true for $Na_V1.2$ and $Na_V1.6$ currents (Ben-Shalom et al., 2017;
292 Hawkins et al., 2011; Martin et al., 2007). $Na_V1.2$ and $Na_V1.6$ are more highly expressed in
293 excitatory neurons (Catterall et al., 2010; Du et al., 2020; Encinas et al., 2020).

294 Additionally, these nonselective agents can block the channels associated with skeletal muscle
295 ($Na_V1.4$), cardiac tissue ($Na_V1.5$), and peripheral neurons ($Na_V1.7$, $Na_V1.8$, $Na_V1.9$). Inhibiting

bioRxiv preprint doi: https://doi.org/10.1101/2021.08.29.458125; this version posted August 31, 2021. The copyright holder for this preprint (which was not certified by peer review) is the author/funder, who has granted bioRxiv a license to display the preprint in perpetuity. It is made available under aCC-BY 4.0 International license.

these off-target channels can compromise muscular, cardiovascular, and sensory function. These risks are highlighted by the FDA's recent drug-safety communication for the nonselective Na_V inhibitor ASM lamotrigine. Lamotrigine has been linked to cardiac liabilities as a consequence of $Na_V1.5$ inhibition (FDA, 2021). Likewise, Na_V inhibitors intended as local anesthetics for trigeminal neuralgia or other pain syndromes and class I cardiac antiarrhythmic drugs are often dose limited by CNS adverse events like dizziness, sedation, and cognitive or motor impairment caused by inhibition of central nervous system Na_V channels (Caron & Libersa, 1997).

An obvious solution to this isoform selectivity challenge is to pursue a precision-medicine approach and create selective pharmacologic agents that preferentially target the sodium channels specific to the desired target tissue or cell type. This selective approach has been pursued for multiple channel isoforms - particularly for the peripheral Na_Vs associated with pain ($Na_V1.3$, $Na_V1.7$, and $Na_V1.8$). This approach has proven challenging because the nine isoforms of sodium channels, $Na_V1.1$-$Na_V1.9$, share a high degree of primary and tertiary structural homology. Achieving selectivity with compounds that have tractable pharmaceutical properties has been particularly difficult.

Previous attempts to optimize Na_V inhibitors for epilepsy have focused on either drug properties or channel-state dependence. To our knowledge, this is the first description of a centrally penetrant, isoform-selective Na_V inhibitor for use in CNS indications, including epilepsy. NBI-921352 represents the first selective inhibitor of $Na_V1.6$ that is suitable for systemic oral administration.

bioRxiv preprint doi: https://doi.org/10.1101/2021.08.29.458125; this version posted August 31, 2021. The copyright holder for this preprint (which was not certified by peer review) is the author/funder, who has granted bioRxiv a license to display the preprint in perpetuity. It is made available under aCC-BY 4.0 International license.

317 The $Na_V1.6$ selective profile of NBI-921352 was designed to inhibit activity in excitatory neurons
318 while sparing firing in the inhibitory interneurons where $Na_V1.1$ is preferentially expressed. We
319 found that NBI-921352 did, in fact, reduce firing in cortical excitatory pyramidal cells. In
320 contrast, inhibitory interneuron firing was not impaired and was seen to increase slightly. The
321 reason for an increase in interneuron action-potential firing is unclear. We propose that this
322 may be a consequence of network effects that arise from interactions with other neurons
323 synapsed onto the target neurons in the experiment. These data confirm that selective $Na_V1.6$
324 inhibitors can distinguish neuronal subtypes in a way that nonselective inhibitors, like
325 carbamazepine, cannot.

326 *SCN8A*-RES patients most often carry de novo genetic variants. While some variants are known
327 to be recurrent, many variants are represented by a single patient (Meisler, 2019). We
328 therefore wanted to assure that NBI-921352 inhibition was not limited to wild-type $Na_V1.6$
329 channels. We tested 9 distinct, patient-identified variants and found that 8 of them were
330 inhibited by NBI-921352 at very similar concentrations as wild-type channels (Figure 2). One
331 variant, R1617Q, was found to be 6.8-fold less sensitive to inhibition than the wild-type
332 channel. R1617Q has been identified in multiple *SCN8A*-DEE patients and is in the domain IV
333 voltage-sensor domain (VSD4). NBI-921352 is an aryl sulfonamide with structural similarity to
334 the $Na_V1.7$ targeted aryl sulfonamides where the binding site has been identified as the $Na_V1.7$
335 VSD4 (Ahuja et al., 2015; McCormack et al., 2013). It is likely that the R1617Q directly or
336 allosterically impairs the tight association of NBI-921252 with $Na_V1.6$ due to its proximity to the
337 binding site. Despite this, NBI-921352 remains markedly more potent than existing Na_V inhibitor
338 drugs on the N1617Q variant $Na_V1.6$ channel. This would suggest that while NBI-921352 may be

bioRxiv preprint doi: https://doi.org/10.1101/2021.08.29.458125; this version posted August 31, 2021. The copyright holder for this preprint (which was not certified by peer review) is the author/funder, who has granted bioRxiv a license to display the preprint in perpetuity. It is made available under aCC-BY 4.0 International license.

339 an effective treatment for *SCN8A*-DEE patients carrying R1617Q variants, higher plasma levels
340 of the compound could be required for efficacy in those patients.

341 Many *SCN8A*-RES associated variants produce their GoF effects by disrupting or destabilizing
342 the inactivation-gating machinery of $Na_V1.6$ channels. This can lead to pathological persistent or
343 resurgent currents that contribute to neuronal hyperexcitability (Pan and Cummins, 2020).

344 Most known small molecule inhibitors of Na_V channels, except some marine toxins like
345 tetrodotoxin, bind preferentially to inactivated or open gating states of the channels and
346 stabilize the channels in inactivated, non-conductive conformations. This state dependence is
347 manifested as a protocol dependence of the apparent drug potency. State dependence
348 inhibition has been described in many ways. Use-dependent, frequency-dependent, resurgent
349 current -selective, and persistent current-selective inhibition are all consequences of a
350 preference for binding to inactivated and/or open channels. Stabilizing inactivated states of the
351 channel reduces persistent and resurgent currents, and this feature has been suggested to
352 contribute to the efficacy of many Na_V targeted ASMs including phenytoin, carbamazepine,
353 oxcarbazepine, lacosamide, cannabidiol, and lamotrigine (Wengert and Patel, 2021). NBI-
354 921352 is also highly state dependent, with a >750-fold preference for open and inactivated
355 channels vs. rested, closed-state channels (sometimes referred to as *peak current*). Forcing all
356 $Na_V1.6$ channels into the closed state by applying voltages more hyperpolarized than
357 physiological (-140 mV) results in very weak inhibition of the channels (Figure 3). Biasing the
358 channels toward activated states (open or inactivated states) by holding the membrane
359 potential more positive in a protocol designed to monitor inactivated state, resurgent current,
360 or persistent current protocol yields potent inhibition. In physiologic conditions, channels are

bioRxiv preprint doi: https://doi.org/10.1101/2021.08.29.458125; this version posted August 31, 2021. The copyright holder for this preprint (which was not certified by peer review) is the author/funder, who has granted bioRxiv a license to display the preprint in perpetuity. It is made available under aCC-BY 4.0 International license.

361 distributed among closed, open, and inactivated states, thus allowing equilibration of potent
362 inhibition of the channel by NBI-921352.

363 Increasing the selectivity of a Na_V inhibitor provides the expectation of an improved safety
364 profile by reducing adverse events caused by off-target activity. An inherent risk of this
365 approach is the potential loss of efficacy that could come from reduced polypharmacy. We have
366 developed a potent, highly selective $Na_V1.6$ inhibitor in NBI-921352. Our studies with NBI-
367 921352 indicate that a $Na_V1.6$ specific compound can retain a robust ability to prevent seizures
368 in rodent models at modest plasma and brain concentrations, consistent with the important
369 role of $Na_V1.6$ in seizure pathways. Our data also suggests that this selectivity profile does
370 improve the tolerability of NBI-921352 relative to commonly employed nonselective sodium
371 channel ASMs in rodents. Whether these results will translate to humans is not yet established,
372 but Phase I clinical trials have shown that NBI-921352 was well tolerated at plasma
373 concentrations higher than were required for efficacy in the preclinical rodent studies described
374 here. NBI-921352 is currently being developed for both *SCN8A*-DEE epilepsy and adult focal-
375 onset seizures by Neurocrine Biosciences (Neurocrine, 2019). Phase II clinical trials will soon
376 evaluate the efficacy of NBI-921352 in patients (Neurocrine, 2021). These clinical trials will
377 provide the first evidence for whether the robust efficacy and tolerability demonstrated in
378 rodents translates to human epilepsy patients.

379

bioRxiv preprint doi: https://doi.org/10.1101/2021.08.29.458125; this version posted August 31, 2021. The copyright holder for this preprint (which was not certified by peer review) is the author/funder, who has granted bioRxiv a license to display the preprint in perpetuity. It is made available under aCC-BY 4.0 International license.

Materials and Methods

Electrophysiological determination of potency and selectivity

Cell lines

Electrophysiology experiments were performed with HEK293 cells either stably transfected or transiently transfected. The stable cell lines were transfected with an expression vector containing the full-length cDNA coding for specific human and mouse sodium channel α-subunit, grown in culture media containing 10% fetal bovine serum, and 0.5 mg/mL Geneticin (G418) at 37°C with 5% CO_2. The $Na_V1.x$ stable cell lines and accessory constructs used correspond to the following GenBank accession numbers: Human $Na_V1.1$ (NM_006920); mouse $Na_V1.1$ (NM_018733.2); human $Na_V1.2$ (NM_021007); mouse $Na_V1.2$ (NP_001092768.1); human $Na_V1.5$ (NM_198056); human $Na_V1.6$ (NM_014191); mouse $Na_V1.6$ (NM_001077499); human $Na_V1.7$ (NM_002977); human $Na_V1.4$ (NM_000334); human $Na_V1.3$ (NM_0069220). The human Na_V β1 subunit (NM_199037) was co-expressed in all cell lines. Human and mouse $Na_V1.6$ channels were also coexpressed with human FHF2B (NM_033642) to increase functional expression. Human $Na_V1.2$ channels were also coexpressed with Contactin 1 (NM_001843) to increase functional expression.

For studies of mutant channels, cDNA plasmids in pcDNA™4/TO Mammalian Expression Vector were transiently transfected into Expi293F™ cells stably expressing human FHF2b and human SCN1B subunit (polyclonal) background using ExpiFectamine™ 293 Transfection Kits (Gibco,Thermo Fisher Scientific CAT #: A14524). Induction was achieved using Tetracycline (Sigma Aldrich). Transfected cells were used in automated patch-clamp experiments 24 hours postinduction.

bioRxiv preprint doi: https://doi.org/10.1101/2021.08.29.458125; this version posted August 31, 2021. The copyright holder for this preprint (which was not certified by peer review) is the author/funder, who has granted bioRxiv a license to display the preprint in perpetuity. It is made available under aCC-BY 4.0 International license.

Na_V channel automated planar patch-clamp assay

NBI-921352 requires several seconds to equilibrate with activated channels, and this property of the compound must be taken into consideration in the design of state-dependent assay voltage-clamp protocols.

Data was collected using the Qube 384 (Sophion) automated voltage-clamp platform using single hole plates. To measure inactivated state inhibition, the membrane potential was maintained at a voltage where inactivation is complete. For each Na_V channel subtype, the V_h used to quantify compound inhibition were as follows: $Na_V1.6$ (-45 mV), $Na_V1.1$ (-45 mV), $Na_V1.2$ (-45 mV), $Na_V1.3$ (-45 mV), $Na_V1.5$ (-60 mV), $Na_V1.7$ (-60 mV), $Na_V1.4$ (-45 mV). The mutant channel $hNa_V1.6^{N1768D}$ was found to have accelerated run-down compared with wild-type $hNa_V1.6$, so the holding potential was adjusted to -60 mV to provide sufficient signal window. The voltage was briefly repolarized to a negative voltage (-150 mV) for 20 milliseconds for ($Na_V1.5$, $Na_V1.7$, $Na_V1.3$, $Na_V1.4$) or for 60 milliseconds (for $Na_V1.1$, $Na_V1.2$, and $Na_V1.6$) to allow recovery from fast inactivation, followed by a test pulse to -20 or 0 mV for 10 milliseconds to quantify the compound inhibition. The repolarization step allows compound-free channels to recover from fast inactivation, but compound-bound channels remain inhibited during the subsequent test step. For rested state "Peak" current V_h was set to -120 mV. Appropriate filters for minimum seal resistance were applied (typically >500 MΩ membrane resistance), and series resistance was compensated at 100%. The pulse protocols were run at 1 Hz for $hNa_V1.7$, $hNa_V1.5$, $hNa_V1.3$, and $hNa_V1.4$ or 0.04 Hz for $Na_V1.6$, $Na_V1.1$ and $Na_V1.2$.

To construct concentration response curves, baseline currents were established after 20 minutes in vehicle (0.5% DMSO). Full inhibition response amplitudes were determined by adding tetrodotoxin (TTX, 300 nM) or tetracaine for $Na_V1.5$ (10 µM) to each well at the end of the experiment. Compounds were then exposed at a single concentration for 20 minutes. One-sixth of every experimental plate was

bioRxiv preprint doi: https://doi.org/10.1101/2021.08.29.458125; this version posted August 31, 2021. The copyright holder for this preprint (which was not certified by peer review) is the author/funder, who has granted bioRxiv a license to display the preprint in perpetuity. It is made available under aCC-BY 4.0 International license.

dedicated to vehicle-only wells that enabled correction for nonspecific drift (i.e., rundown) of the signal in each experiment. For all channel subtypes, inhibition by the compound reached steady state within 20 minutes of incubation. The current inhibition values ($I_{(CPD)}$) were normalized to both the vehicle ($I_{control}$) and the full response defined by supramaximal TTX (I_{TTX}) or tetracaine (for $Na_V1.5$) addition responses according to Equation 1:

Equation 1

$$I_{norm(CPD)} = (I_{CPD} - I_{control})/(I_{TTX} - I_{control}).$$

This normalized inhibition was then further normalized to the span of the assay to account for the run-down seen in cells exposed to vehicle alone for 20 minutes as follows:

Equation 2

$$I_{norm,\ span} = (I_{norm(CPD)} - I_{norm(VEH)}) / (1 - I_{norm(VEH)}),$$

where:

$I_{norm,\ span}$ = the current response normalized to within the span of the assay.

$I_{norm(CPD)}$ = the normalized response in the presence of compound.

$I_{norm(VEH)})$ = the normalized response in the absence of compound.

This normalization ensures that the data ranges were between 0 and 1, and there is no rundown in the plots. The normalized data from all cell recordings at a concentration were grouped together and plotted with GraphPad Prism 8, and IC_{50} values were calculated for grouped data using the following version of the Hill equation:

Equation 3

$$Y = RD + (1 - RD) \times [CPD] / (IC_{50} + [CPD])),$$

bioRxiv preprint doi: https://doi.org/10.1101/2021.08.29.458125; this version posted August 31, 2021. The copyright holder for this preprint (which was not certified by peer review) is the author/funder, who has granted bioRxiv a license to display the preprint in perpetuity. It is made available under aCC-BY 4.0 International license.

where:

Y = the fraction of sodium current blocked in the presence of the compound.

[CPD] = the concentration of compound.

IC_{50} = the IC_{50} concentration.

RD = the "rundown" of sodium current in vehicle alone, which is equal to 0 in this case, as the inhibition has already been normalized to the span.

The Hill slope was fixed to 1.

The 95% CI for the IC_{50} from the fitted curve to the mean data were reported unless otherwise noted.

To evaluate inhibition of hNa_V1.6(N1768D) resurgent currents, synthetic $Na_V\beta$4 peptide (KKLITFILKKTREKKKECLV) was added to the intracellular recording solution at 200 µM and a dedicated protocol to elicit resurgent currents was employed (Barbosa et al., 2015). Cells were voltage clamped at (V_h = -80 mV) and subjected to a strong depolarization (+60 mV) for 20 milliseconds. Following the strong depolarization, cells were partially repolarized to the voltage where resurgent current was maximal (-20 mV) for 50 milliseconds, and resurgent current amplitude was measured. This resurgent current-specific waveform was repeated at 5 Hz for 100 s in vehicle, followed by 100 s in test compound, then 300 nM TTX. Fractional inhibition was calculated using the same normalization procedure as above.

Experiments were all performed at 27°C ± 2°C.

Automated patch-clamp recording solutions

The recording solutions for Na_V1.1, Na_V1.2, Na_V1.3, Na_V1.4 and Na_V1.6 cell line studies contained:

Intracellular solution (ICS): 5 mM NaCl, 10 mM CsCl, 120 mM CsF, 0.1 mM $CaCl_2$, 2 mM $MgCl_2$, 10 mM

bioRxiv preprint doi: https://doi.org/10.1101/2021.08.29.458125; this version posted August 31, 2021. The copyright holder for this preprint (which was not certified by peer review) is the author/funder, who has granted bioRxiv a license to display the preprint in perpetuity. It is made available under aCC-BY 4.0 International license.

HEPES (4-(2-hydroxyethyl)-1-piperazineethanesulfonic acid buffer), 10 mM EGTA (ethylene glycol tetraacetic acid); adjusted to pH 7.2 with CsOH. Extracellular solution (ECS): 140 mM NaCl, 5 mM KCl, 2 mM $CaCl_2$, 1 mM $MgCl_2$, 10 mM HEPES; adjusted to pH 7.4 with NaOH. Solutions with a reversed Na^+ gradient were used for $Na_V1.5$ and $Na_V1.7$ studies since they improved technical success. ICS: 120 mM NaF, 10 mM CsCl, 0.1 mM $CaCl_2$, 2 mM $MgCl_2$, 10 mM HEPES, 10 mM EGTA; adjusted to pH 7.2 with CsOH. ECS: 1 mM NaCl, 139 mM CholineCl, 5 mM KCl, 2 mM $CaCl_2$, 1 mM $MgCl_2$, 10 mM HEPES; adjusted to pH 7.4 with NaOH. Osmolarity in all ICS and ECS solutions was adjusted with glucose to 300 mOsm/kg and 310 mOsm/kg, respectively.

Current-clamp recording of cortical pyramidal neurons and inhibitory interneurons

Slice preparation

Parasagittal cortical brain slices were prepared from >P21 mice using standard procedures (adapted from Tai et al., PNAS 2014). Briefly, the mouse was deeply anaesthetized with isoflurane and decapitated. The brain was removed and placed into chilled artificial cerebrospinal fluid (aCSF) solution containing (in mM): 125 NaCl, 25 NaHCO3, 2.5 KCl, 1.25 NaH_2PO_4, 2 $CaCl_2$, 2 $MgCl_2$, 10 d-glucose, pH 7.3, osmolarity adjusted to ~306 mOsm using sucrose. All solutions were saturated with 95% O_2 and 5% CO_2 constantly perfused with 95% O_2/5% CO_2. Slices with a thickness of 400 µm were prepared using a vibratome (Ted Pella, Inc.). Following sectioning, the slices were placed in a holding chamber and incubated in a water bath at 34°C for 15 minutes. The brain slices were removed from the water bath and held at room temperature for 60 minutes prior to recording.

Brain slice electrophysiology assay

All experiments involving rodent subjects were performed in accordance with the guidelines of the Canadian Council on Animal Care (CCAC). Following a 60-minute incubation at room temperature, a brain slice was selected and placed on the stage of an upright microscope (SliceScope Pro 2000,

bioRxiv preprint doi: https://doi.org/10.1101/2021.08.29.458125; this version posted August 31, 2021. The copyright holder for this preprint (which was not certified by peer review) is the author/funder, who has granted bioRxiv a license to display the preprint in perpetuity. It is made available under aCC-BY 4.0 International license.

Scientifica). The slice was constantly perfused with room temperature aCSF, containing 0.1% DMSO as a vehicle control, and oxygenated with 95% O_2/5% CO_2.The slice was visualized using brightfield microscopy, and a healthy neuron was selected from neocortical layer 5. Whole-cell configuration was achieved with a pipette (bath resistance 4 – 6 MΩ) containing internal solution. Stimulation was applied in current-clamp mode, and consisted of a series of 1000 ms square pulses, beginning at -20 pA and increasing by +20 pA increments (3000 ms between pulses).

Once the recordings in vehicle were completed, and while still holding the patch on the same neuron, the bath solution was changed from 0.1% DMSO in aCSF to 0.25 µM NBI-921352 or 100 µM Carbamazepine in aCSF. The slice was incubated in circulating compound for 10 minutes before repeating the series of square pulse stimulations. Working stock solutions were prepared in DMSO at a concentration of 20 mM.

All data analysis was done offline using ClampFit 10.7 (Molecular Devices). Data are presented as a mean ± SEM. For each sweep, the number of evoked APs was counted, and plotted as a function of current injection (beginning with -20 pA). These generated “input/output” (or “F/I”) curves demonstrating the relationship between stimulus and average AP frequency. Statistical significance was assessed using paired, two-way, student’s t-test applied at each current injection level with significance considered $P<0.05$.

Formulation and oral dosing of NBI-921352

Vehicle preparation

The vehicle for oral dosing solutions was 0.5% methyl cellulose and 0.2% Tween-80 in deionized (DI) water. DI water (0.8 L) was heated up to 70°C to 80°C. Five grams of methyl cellulose was slowly added to heated DI water. The mixture was stirred until it formed a homogeneous milky suspension. The suspension was moved to a cold room and stirred overnight to get a clear solution. Two milliliters of

bioRxiv preprint doi: https://doi.org/10.1101/2021.08.29.458125; this version posted August 31, 2021. The copyright holder for this preprint (which was not certified by peer review) is the author/funder, who has granted bioRxiv a license to display the preprint in perpetuity. It is made available under aCC-BY 4.0 International license.

Tween-80 was added to the clear solution and diluted up to 1 L with DI water. The vehicle solution was stored at 2°C to 8°C.

Drug formulation

NBI-921352 was weighed into vials. An appropriate amount of vehicle was added to the NBI-921352 powder then mixed on a T18 ULTRA TURRAX homogenizer (IKA, Wilmington, NC) to create a uniform suspension at the desired concentration. The vials were then wrapped in aluminum foil to protect them from light and placed on a stir plate until the time of dosing. Carbamazepine and lacosamide were formulated in the same manner. Phenytoin was formulated in 0.9% physiological saline.

Dosing

NBI-921352, carbamazepine, and lacosamide were administered orally using a stainless-steel gavage needle at a dose volume of 10 ml/kg. Phenytoin was formulated in physiologic saline and was administered intraperitoneally (i.p.) using a 25-gauge needle at a dose volume of 10 mL/kg. All compounds were administered 2 hours prior to electrical seizure induction for all seizure models employed in this study.

Bioanalytical assessment of plasma and brain concentrations

Sample collection: Approximately 0.5 mL of blood was collected from each mouse at the end of the assay via cardiac puncture under deep anesthesia. The blood samples were collected in a syringe and transferred to tubes containing EDTA. Blood was stored at 4°C until centrifuged within 30 minutes of collection. Plasma was harvested and placed on dry ice and stored in a freezer set to maintain a temperature of -70°C to -80°C until analysis. Brains were harvested immediately after blood collection and placed on dry ice prior to storage in a freezer set to maintain a temperature of -70°C to -80°C until analysis.

bioRxiv preprint doi: https://doi.org/10.1101/2021.08.29.458125; this version posted August 31, 2021. The copyright holder for this preprint (which was not certified by peer review) is the author/funder, who has granted bioRxiv a license to display the preprint in perpetuity. It is made available under aCC-BY 4.0 International license.

Plasma samples: Extraction of plasma samples was carried out by protein precipitation using acetonitrile. Plasma samples (50 µL) were mixed with 50 µL of internal standard (IS) solution in water followed by addition of 10 µL of concentrated ortho-phosphoric acid and 200 µL of acetonitrile. Samples were vortexed for 30 seconds, centrifuged at 13,000 rpm for 20 minutes, decanted in to a 96-well plate, and further centrifuged at 4,000 rpm for 20 minutes. The samples were analyzed by UHPLC-ESI-MS/MS as described below.

Brain samples: Prior to extraction, pre-weighed whole brains were homogenized in 1:1 acetonitrile/water (v/v) (4 mL per mouse brain) using an IKA T18 ULTRA-TURRAX Homogenizer at the setting of 4 for approximately 2 min. The homogenate was centrifuged at 13,000 rpm for 20 min and 50 µL of the supernatant were treated exactly as described above for plasma samples. 50 µL of the brain homogenate were then treated exactly as the plasma samples described above.

Standards and quality control (QC) samples: K_2EDTA Blank mouse plasma purchased from Valley Biomedical, California, USA was used to prepare standards and QC samples for plasma quantitation and as surrogates for brain homogenate quantitation. Calibration samples ranged from 2.34 ng/mL to 4,800 ng/mL. QC samples concentration included 14 ng/mL (QC-L), 255 ng/mL (QC-M) and 3,600 ng/mL (QC-H). Standards and QC samples were processed the same way as the sample extracts described above.

Analytical methods and statistics for plasma and tissue samples:

Samples were analyzed by UHPLC-ESI MS/MS using a TQ-5500 Sciex triple quadrupole mass spectrometer equipped with a Shimadzu Nexera UHPLC pump and auto-sampler system using an ACE C18 PFP, 2.50 x 50 mm, 1.7 µ particle size column and gradient elution consisting of solvent A (0.1%

bioRxiv preprint doi: https://doi.org/10.1101/2021.08.29.458125; this version posted August 31, 2021. The copyright holder for this preprint (which was not certified by peer review) is the author/funder, who has granted bioRxiv a license to display the preprint in perpetuity. It is made available under aCC-BY 4.0 International license.

formic acid in water) and solvent B (0.1% formic acid in acetonitrile) starting at 20% B from 0 min to 0.4 min and then increased to 100% B from 0.4 min to 0.6 min. At 2.0 min, the mobile phase composition was switched back to 60% B for 1 min. The flow rate used throughout the experiment was 0.4 min/mL. The analyte, NBI-921352, and the IS were detected by electrospray in the positive ion mode using the following transitions: m/z 460/91 for NBI-921352 and m/z 503/341m/z for the IS. The UHPLC-ESI MS/MS system was controlled by Analyst 1.6.

Sample concentrations were determined using a linear calibration function, weighted 1/X, generated by the regression of analyte to IS peak area ratios in the standard samples to their respective concentrations. Acceptance criteria for the analytical run required that the back calculated values of the standards and the QC samples fell within ± 20% of their nominal values, except for the lowest standard or lower limit of quantitation (LLOQ), for which the acceptance criterion was ± 25%. At least 6 out of 12 standard points had to show back-calculated values within ± 20% of their nominal concentrations for the calibration to be accepted. At least three QC samples, one at each level, had to show back-calculated values within ± 20% of their nominal concentrations for the whole sample batch to be valid.

Animals

After delivery, animals were allowed sufficient time to acclimate prior to testing (~1 week). All animals were housed in plastic cages in rooms with controlled humidity, ventilation, and lighting (12 hr/12 hr light–dark cycle). All animal procedures were performed using protocols approved by Xenon Animal Care Committee and the Canadian Council on Animal Care.

Scn8aN1768D/+ mice:

Xenon Pharmaceuticals Inc. licensed the mouse with the missense mutation p.Asn1768Asp (N1768D) in the neuronal sodium channel $Na_V1.6$, characterized and developed by Dr. M Meisler (University Of Michigan, MI, USA). The *Scn8a*^{N1768D} knock-in allele was generated by TALEN targeting of (C57BL/6JXSJL)

bioRxiv preprint doi: https://doi.org/10.1101/2021.08.29.458125; this version posted August 31, 2021. The copyright holder for this preprint (which was not certified by peer review) is the author/funder, who has granted bioRxiv a license to display the preprint in perpetuity. It is made available under aCC-BY 4.0 International license.

F2 eggs at the University of Michigan Transgenic Animal Model Core. The line was propagated by backcrossing N1768D/+ heterozygotes to C57BL/6J wild-type mice (The Jackson Laboratory, Bar Harbor, ME). Male N1768D/+ heterozygotes on a C57BL/6J background were subsequently backcrossed to C3HeB/FeJ female mice. All the experiments were performed using animals following at least 7 such backcrosses. Experiments were performed using (B6 × C3He) F7 (F7. N1768D/+) offspring aged 35-42 days.

WT mice:

Adult male CF-1 WT albino mice 26-35 g were obtained from Charles River, Senneville, Quebec, Canada. All the assays were carried out in mice 9 weeks or older.

Sprague-Dawley rats:

Adult male Sprague-Dawley albino rats weighing 150-200 g were obtained from Envigo, Livermore, CA, USA. All the assays were carried out in rats 5 weeks or older.

The modified 6 Hz psychomotor seizure assay

The modified 6 Hz seizure assay in *Scn8a*$^{N1768D/+}$ heterozygous mice was adapted from the traditional 6 Hz assay psychomotor seizure assay to provide a measure of in vivo on target ($Na_V1.6$ mediated) efficacy (Barton et al., 2001). The modified assay used a low frequency (6 Hz) but long-duration stimulation (3 seconds) to induce seizures. We identified 12 mA and a 0.3 millisecond pulse interval as a suitable current for testing in *Scn8a*$^{N1768D/+}$ mice, since it differentiated mutant and wild-type (WT) mice. An electroshock (6 Hz, 12 mA) was delivered for 3 seconds (at 0.3 millisecond pulse interval) by corneal electrodes (Electro Convulsive Therapy Unit 57800 from Ugo Basile). Immediately prior to the electroshock, the animals' eyes were anesthetized with a drop of Alcaine (0.5% proparacaine hydrochloride). Upon corneal

bioRxiv preprint doi: https://doi.org/10.1101/2021.08.29.458125; this version posted August 31, 2021. The copyright holder for this preprint (which was not certified by peer review) is the author/funder, who has granted bioRxiv a license to display the preprint in perpetuity. It is made available under aCC-BY 4.0 International license.

stimulation, WT mice experienced mild seizure behaviors such as facial clonus, forelimb clonus, Straub tail, rearing, and falling, but did not experience a generalized tonic-clonic seizure (GTC) with hindlimb extension. *Scn8a*$^{N1768D/+}$ animals, however, in addition to mild seizure behaviors, experienced a GTC with hindlimb extension. The modified assay showed a clear differentiation of seizure behavior between WT and *Scn8a*$^{N1768D/+}$ mice. *Scn8a*$^{N1768D/+}$ mice exhibited GTC with hindlimb extension but not WT mice.

For the single-dose and repeated-dose efficacy experiments, *Scn8a*$^{N1768D/+}$ animals were dosed PO with vehicle or NBI-921352 two hours before the administration of the electric stimulation. An animal was considered protected in the assay upon prevention of GTC with hindlimb extension and was then scored “0”. An animal displaying GTC with hindlimb extension was considered not protected and is then scored “1”. The experimenter scoring the seizure behavior was blinded to the treatment.

DC-Maximal electroshock seizure assay in rodents

The maximal electroshock seizure (MES) assay has been extensively used in the search for anticonvulsant substances (Loscher et al., 1991; Piredda et al., 1985; White et al., 1995). The MES assay is sensitive to nonselective NaV inhibitors. It is considered a model for generalized tonic-clonic (GTC) seizures and provides an assessment of seizure spread. Briefly, an electroshock of direct current (DC) was delivered by corneal electrodes (Electro Convulsive Therapy Unit 57800 from Ugo Basile). The parameters of stimulation were different between mice and rats. In CF1 mice, a direct current of 50 mA (60 Hz) was delivered for 0.2 seconds (pulse width of 0.5 ms), whereas in Sprague Dawley (SD) rats, a direct current of 150 mA (60 Hz) was delivered for 0.3 seconds (pulse width of 0.5 ms). Immediately prior to the electroshock,

bioRxiv preprint doi: https://doi.org/10.1101/2021.08.29.458125; this version posted August 31, 2021. The copyright holder for this preprint (which was not certified by peer review) is the author/funder, who has granted bioRxiv a license to display the preprint in perpetuity. It is made available under aCC-BY 4.0 International license.

the animals' eyes were anesthetized with a drop of Alcaine (0.5% proparacaine hydrochloride). Upon corneal stimulation, naïve animals experienced a generalized tonic-clonic seizure (GTC) with hindlimb extension.

For the efficacy experiments, single dose and repeated dose, animals were dosed PO with vehicle or NBI-921352 two hours before the administration of the electric stimulation. An animal was considered protected in the assay in the absence of a GTC with hindlimb extension and is then scored "0". An animal displaying GTC with hindlimb extension was considered not protected and is then scored "1". The experimenter scoring the seizure behavior was blinded to the treatment.

Blinding of in vivo efficacy experiments

On each testing day, individual treatment groups were assigned a random label (e.g., A, B, C, etc.) by the technical staff administering the compound. To ensure blinding, the technical staff member performing drug administration differed from the person performing the test. Therefore, the experimenter conducting testing was blinded to treatment group (e.g., drug or vehicle treatment, dose, and time point).

Randomization of in vivo efficacy experiments

Randomization of animals into various treatment groups occurred on a per-animal (e.g., rather than a per-cage) basis. Therefore, each animal was randomly assigned to a treatment group, and all animals tested in each experiment had an equal chance of assignment to any treatment group. Prior to each study, a randomization sequence was obtained (www.graphpad.com/quickcalcs).

bioRxiv preprint doi: https://doi.org/10.1101/2021.08.29.458125; this version posted August 31, 2021. The copyright holder for this preprint (which was not certified by peer review) is the author/funder, who has granted bioRxiv a license to display the preprint in perpetuity. It is made available under aCC-BY 4.0 International license.

Acknowledgements

We thank Dr. Fiona Scott, PhD of Neurocrine Biosciences for thoughtful discussions and commentary on this manuscript. We thank Ian Mortimer of Xenon Pharmaceuticals for strategic discussions. We thank Dr. Miriam Meisler, PhD for making *Scn8a*$^{N1768D/+}$ mice available. We thank the *SCN8A*-RES patients, families and patient advocates for detailed discussions regarding the clinical presentation of *SCN8A* mutations and unmet medical needs in their community.

Competing Interests

All authors are, or were previously, employees of Xenon Pharmaceuticals Inc. They receive or received salaries from Xenon Pharmaceuticals Inc. and may hold stock or stock options in Xenon Pharmaceuticals Inc.

bioRxiv preprint doi: https://doi.org/10.1101/2021.08.29.458125; this version posted August 31, 2021. The copyright holder for this preprint (which was not certified by peer review) is the author/funder, who has granted bioRxiv a license to display the preprint in perpetuity. It is made available under aCC-BY 4.0 International license.

References

Ahuja, S., Mukund, S., Deng, L., Khakh, K., Chang, E., Ho, H., . . . Payandeh, J. (2015). Structural basis of Nav1.7 inhibition by an isoform-selective small-molecule antagonist. *Science, 350*(6267), aac5464. doi:10.1126/science.aac5464

Barbosa, C., Tan, Z. Y., Wang, R., Xie, W., Strong, J. A., Patel, R. R., . . . Cummins, T. R. (2015). Navbeta4 regulates fast resurgent sodium currents and excitability in sensory neurons. *Mol Pain, 11*, 60. doi:10.1186/s12990-015-0063-9

Barton, M. E., Klein, B. D., Wolf, H. H., & White, H. S. (2001). Pharmacological characterization of the 6 Hz psychomotor seizure model of partial epilepsy. *Epilepsy Res, 47*(3), 217-227. doi:10.1016/s0920-1211(01)00302-3

Bean, B. P., Cohen, C. J., & Tsien, R. W. (1983). Lidocaine block of cardiac sodium channels. *J Gen Physiol, 81*(5), 613-642. doi:10.1085/jgp.81.5.613

Ben-Shalom, R., Keeshen, C. M., Berrios, K. N., An, J. Y., Sanders, S. J., & Bender, K. J. (2017). Opposing Effects on NaV1.2 Function Underlie Differences Between SCN2A Variants Observed in Individuals With Autism Spectrum Disorder or Infantile Seizures. *Biol Psychiatry, 82*(3), 224-232. doi:10.1016/j.biopsych.2017.01.009

Boerma, R. S., Braun, K. P., van de Broek, M. P., van Berkestijn, F. M., Swinkels, M. E., Hagebeuk, E. O., . . . Koeleman, B. P. (2016). Remarkable Phenytoin Sensitivity in 4 Children with SCN8A-related Epilepsy: A Molecular Neuropharmacological Approach. *Neurotherapeutics, 13*(1), 192-197. doi:10.1007/s13311-015-0372-8

Braakman, H. M., Verhoeven, J. S., Erasmus, C. E., Haaxma, C. A., Willemsen, M. H., & Schelhaas, H. J. (2017). Phenytoin as a last-resort treatment in SCN8A encephalopathy. *Epilepsia Open, 2*(3), 343-344. doi:10.1002/epi4.12059

bioRxiv preprint doi: https://doi.org/10.1101/2021.08.29.458125; this version posted August 31, 2021. The copyright holder for this preprint (which was not certified by peer review) is the author/funder, who has granted bioRxiv a license to display the preprint in perpetuity. It is made available under aCC-BY 4.0 International license.

680 Burgess, D. L., Kohrman, D. C., Galt, J., Plummer, N. W., Jones, J. M., Spear, B., & Meisler, M. H. (1995).
681 Mutation of a new sodium channel gene, Scn8a, in the mouse mutant 'motor endplate disease'.
682 *Nat Genet, 10*(4), 461-465. doi:10.1038/ng0895-461
683 Caron, J., & Libersa, C. (1997). Adverse effects of class I antiarrhythmic drugs. *Drug Saf, 17*(1), 8-36.
684 doi:10.2165/00002018-199717010-00002
685 Catterall, W. A., Kalume, F., & Oakley, J. C. (2010). NaV1.1 channels and epilepsy. *J Physiol, 588*(Pt 11),
686 1849-1859. doi:10.1113/jphysiol.2010.187484
687 Chen, Q., Kirsch, G. E., Zhang, D., Brugada, R., Brugada, J., Brugada, P., . . . Wang, Q. (1998). Genetic basis
688 and molecular mechanism for idiopathic ventricular fibrillation. *Nature, 392*(6673), 293-296.
689 doi:10.1038/32675
690 Claes, L., Del-Favero, J., Ceulemans, B., Lagae, L., Van Broeckhoven, C., & De Jonghe, P. (2001). De novo
691 mutations in the sodium-channel gene SCN1A cause severe myoclonic epilepsy of infancy. *Am J*
692 *Hum Genet, 68*(6), 1327-1332. doi:10.1086/320609
693 Courtney, K. R., Kendig, J. J., & Cohen, E. N. (1978). The rates of interaction of local anesthetics with
694 sodium channels in nerve. *J Pharmacol Exp Ther, 207*(2), 594-604. Retrieved from
695 https://www.ncbi.nlm.nih.gov/pubmed/712641
696 Du, J., Simmons, S., Brunklaus, A., Adiconis, X., Hession, C. C., Fu, Z., . . . Lal, D. (2020). Differential
697 excitatory vs inhibitory SCN expression at single cell level regulates brain sodium channel
698 function in neurodevelopmental disorders. *Eur J Paediatr Neurol, 24*, 129-133.
699 doi:10.1016/j.ejpn.2019.12.019
700 Encinas, A. C., Watkins, J. C., Longoria, I. A., Johnson, J. P., Jr., & Hammer, M. F. (2020). Variable patterns
701 of mutation density among NaV1.1, NaV1.2 and NaV1.6 point to channel-specific functional
702 differences associated with childhood epilepsy. *PLoS One, 15*(8), e0238121.
703 doi:10.1371/journal.pone.0238121

bioRxiv preprint doi: https://doi.org/10.1101/2021.08.29.458125; this version posted August 31, 2021. The copyright holder for this preprint (which was not certified by peer review) is the author/funder, who has granted bioRxiv a license to display the preprint in perpetuity. It is made available under aCC-BY 4.0 International license.

Escayg, A., MacDonald, B. T., Meisler, M. H., Baulac, S., Huberfeld, G., An-Gourfinkel, I., . . . Malafosse, A. (2000). Mutations of SCN1A, encoding a neuronal sodium channel, in two families with GEFS+2. *Nat Genet, 24*(4), 343-345. doi:10.1038/74159

FDA. (2021). *Drug Safety Communication: Studies show increased risk of heart rhythm problems with seizure and mental health medicine lamotrigine (Lamictal) in patients with heart disease*. Retrieved from https://www.fda.gov/drugs/drug-safety-and-availability/studies-show-increased-risk-heart-rhythm-problems-seizure-and-mental-health-medicine-lamotrigine

Focken, T., Burford, K., Grimwood, M. E., Zenova, A., Andrez, J. C., Gong, W., . . . Empfield, J. R. (2019). Identification of CNS-Penetrant Aryl Sulfonamides as Isoform-Selective NaV1.6 Inhibitors with Efficacy in Mouse Models of Epilepsy. *J Med Chem, 62*(21), 9618-9641. doi:10.1021/acs.jmedchem.9b01032

Gardella, E., & Moller, R. S. (2019). Phenotypic and genetic spectrum of SCN8A-related disorders, treatment options, and outcomes. *Epilepsia, 60 Suppl 3*, S77-S85. doi:10.1111/epi.16319

Gennaro, E., Veggiotti, P., Malacarne, M., Madia, F., Cecconi, M., Cardinali, S., . . . Zara, F. (2003). Familial severe myoclonic epilepsy of infancy: truncation of Nav1.1 and genetic heterogeneity. *Epileptic Disord, 5*(1), 21-25. Retrieved from https://www.ncbi.nlm.nih.gov/pubmed/12773292

Hammer, M. F., Wagnon, J. L., Mefford, H. C., & Meisler, M. H. (2016). SCN8A-Related Epilepsy with Encephalopathy. In M. P. Adam, H. H. Ardinger, R. A. Pagon, S. E. Wallace, L. J. H. Bean, K. Stephens, & A. Amemiya (Eds.), *GeneReviews((R))*. Seattle (WA).

Hawkins, N. A., Martin, M. S., Frankel, W. N., Kearney, J. A., & Escayg, A. (2011). Neuronal voltage-gated ion channels are genetic modifiers of generalized epilepsy with febrile seizures plus. *Neurobiol Dis, 41*(3), 655-660. doi:10.1016/j.nbd.2010.11.016

bioRxiv preprint doi: https://doi.org/10.1101/2021.08.29.458125; this version posted August 31, 2021. The copyright holder for this preprint (which was not certified by peer review) is the author/funder, who has granted bioRxiv a license to display the preprint in perpetuity. It is made available under aCC-BY 4.0 International license.

726 Inglis, G. A. S., Wong, J. C., Butler, K. M., Thelin, J. T., Mistretta, O. C., Wu, X., . . . Escayg, A. (2020).
727 Mutations in the Scn8a DIIS4 voltage sensor reveal new distinctions among hypomorphic and
728 null Nav 1.6 sodium channels. *Genes Brain Behav, 19*(4), e12612. doi:10.1111/gbb.12612
729 Johannesen, K. M., Gardella, E., Encinas, A. C., Lehesjoki, A. E., Linnankivi, T., Petersen, M. B., . . . Moller,
730 R. S. (2019). The spectrum of intermediate SCN8A-related epilepsy. *Epilepsia, 60*(5), 830-844.
731 doi:10.1111/epi.14705
732 Liu, Y., Schubert, J., Sonnenberg, L., Helbig, K. L., Hoei-Hansen, C. E., Koko, M., . . . Lerche, H. (2019).
733 Neuronal mechanisms of mutations in SCN8A causing epilepsy or intellectual disability. *Brain,*
734 *142*(2), 376-390. doi:10.1093/brain/awy326
735 Loscher, W., Fassbender, C. P., & Nolting, B. (1991). The role of technical, biological and pharmacological
736 factors in the laboratory evaluation of anticonvulsant drugs. II. Maximal electroshock seizure
737 models. *Epilepsy Res, 8*(2), 79-94. doi:10.1016/0920-1211(91)90075-q
738 Martin, M. S., Tang, B., Papale, L. A., Yu, F. H., Catterall, W. A., & Escayg, A. (2007). The voltage-gated
739 sodium channel Scn8a is a genetic modifier of severe myoclonic epilepsy of infancy. *Hum Mol*
740 *Genet, 16*(23), 2892-2899. doi:10.1093/hmg/ddm248
741 Mason, E. R., Wu, F., Patel, R. R., Xiao, Y., Cannon, S. C., & Cummins, T. R. (2019). Resurgent and Gating
742 Pore Currents Induced by De Novo SCN2A Epilepsy Mutations. *eNeuro, 6*(5).
743 doi:10.1523/ENEURO.0141-19.2019
744 McCormack, K., Santos, S., Chapman, M. L., Krafte, D. S., Marron, B. E., West, C. W., . . . Castle, N. A.
745 (2013). Voltage sensor interaction site for selective small molecule inhibitors of voltage-gated
746 sodium channels. *Proc Natl Acad Sci U S A, 110*(29), E2724-2732. doi:10.1073/pnas.1220844110
747 Meisler, M. H. (2019). SCN8A encephalopathy: Mechanisms and models. *Epilepsia, 60 Suppl 3*, S86-S91.
748 doi:10.1111/epi.14703

bioRxiv preprint doi: https://doi.org/10.1101/2021.08.29.458125; this version posted August 31, 2021. The copyright holder for this preprint (which was not certified by peer review) is the author/funder, who has granted bioRxiv a license to display the preprint in perpetuity. It is made available under aCC-BY 4.0 International license.

749 Mistry, A. M., Thompson, C. H., Miller, A. R., Vanoye, C. G., George, A. L., Jr., & Kearney, J. A. (2014).
750 Strain- and age-dependent hippocampal neuron sodium currents correlate with epilepsy
751 severity in Dravet syndrome mice. *Neurobiol Dis, 65*, 1-11. doi:10.1016/j.nbd.2014.01.006
752 Neurocrine. (2019). Neurocrine Biosciences and Xenon Pharmaceuticals Announce Agreement to
753 Develop First-in-Class Treatments for Epilepsy. *Press Release*. Retrieved from
754 https://neurocrine.gcs-web.com/news-releases/news-release-details/neurocrine-biosciences-
755 and-xenon-pharmaceuticals-announce
756 Neurocrine. (2021). Study to Evaluate NBI-921352 as Adjunctive Therapy in Subjects With SCN8A
757 Developmental and Epileptic Encephalopathy Syndrome (SCN8A-DEE). *ClinicalTrials.gov*
758 Retrieved from
759 https://www.clinicaltrials.gov/ct2/show/NCT04873869?term=NCT04873869&draw=2&rank=1
760 Pan, Y., & Cummins, T. R. (2020). Distinct functional alterations in SCN8A epilepsy mutant channels. *J*
761 *Physiol, 598*(2), 381-401. doi:10.1113/JP278952
762 Piredda, S. G., Woodhead, J. H., & Swinyard, E. A. (1985). Effect of stimulus intensity on the profile of
763 anticonvulsant activity of phenytoin, ethosuximide and valproate. *J Pharmacol Exp Ther, 232*(3),
764 741-745. Retrieved from https://www.ncbi.nlm.nih.gov/pubmed/3919174
765 Potet, F., Egecioglu, D. E., Burridge, P. W., & George, A. L., Jr. (2020). GS-967 and Eleclazine Block Sodium
766 Channels in Human Induced Pluripotent Stem Cell-Derived Cardiomyocytes. *Mol Pharmacol,*
767 *98*(5), 540-547. doi:10.1124/molpharm.120.000048
768 Ptacek, L. J., George, A. L., Jr., Griggs, R. C., Tawil, R., Kallen, R. G., Barchi, R. L., . . . Leppert, M. F. (1991).
769 Identification of a mutation in the gene causing hyperkalemic periodic paralysis. *Cell, 67*(5),
770 1021-1027. doi:10.1016/0092-8674(91)90374-8

bioRxiv preprint doi: https://doi.org/10.1101/2021.08.29.458125; this version posted August 31, 2021. The copyright holder for this preprint (which was not certified by peer review) is the author/funder, who has granted bioRxiv a license to display the preprint in perpetuity. It is made available under aCC-BY 4.0 International license.

771 Raman, I. M., & Bean, B. P. (1997). Resurgent sodium current and action potential formation in
772 dissociated cerebellar Purkinje neurons. *J Neurosci, 17*(12), 4517-4526. Retrieved from
773 https://www.ncbi.nlm.nih.gov/pubmed/9169512
774 Raman, I. M., Sprunger, L. K., Meisler, M. H., & Bean, B. P. (1997). Altered subthreshold sodium currents
775 and disrupted firing patterns in Purkinje neurons of Scn8a mutant mice. *Neuron, 19*(4), 881-891.
776 doi:10.1016/s0896-6273(00)80969-1
777 Rojas, C. V., Wang, J. Z., Schwartz, L. S., Hoffman, E. P., Powell, B. R., & Brown, R. H., Jr. (1991). A Met-to-
778 Val mutation in the skeletal muscle Na+ channel alpha-subunit in hyperkalaemic periodic
779 paralysis. *Nature, 354*(6352), 387-389. doi:10.1038/354387a0
780 Royeck, M., Horstmann, M. T., Remy, S., Reitze, M., Yaari, Y., & Beck, H. (2008). Role of axonal NaV1.6
781 sodium channels in action potential initiation of CA1 pyramidal neurons. *J Neurophysiol, 100*(4),
782 2361-2380. doi:10.1152/jn.90332.2008
783 Strichartz, G. (1976). Molecular mechanisms of nerve block by local anesthetics. *Anesthesiology, 45*(4),
784 421-441. doi:10.1097/00000542-197610000-00012
785 Tidball, A. M., Lopez-Santiago, L. F., Yuan, Y., Glenn, T. W., Margolis, J. L., Clayton Walker, J., . . . Parent,
786 J. M. (2020). Variant-specific changes in persistent or resurgent sodium current in SCN8A-related
787 epilepsy patient-derived neurons. *Brain, 143*(10), 3025-3040. doi:10.1093/brain/awaa247
788 Veeramah, K. R., O'Brien, J. E., Meisler, M. H., Cheng, X., Dib-Hajj, S. D., Waxman, S. G., . . . Hammer, M.
789 F. (2012). De novo pathogenic SCN8A mutation identified by whole-genome sequencing of a
790 family quartet affected by infantile epileptic encephalopathy and SUDEP. *Am J Hum Genet,*
791 *90*(3), 502-510. doi:10.1016/j.ajhg.2012.01.006
792 Wagnon, J. L., Korn, M. J., Parent, R., Tarpey, T. A., Jones, J. M., Hammer, M. F., . . . Meisler, M. H. (2015).
793 Convulsive seizures and SUDEP in a mouse model of SCN8A epileptic encephalopathy. *Hum Mol*
794 *Genet, 24*(2), 506-515. doi:10.1093/hmg/ddu470

bioRxiv preprint doi: https://doi.org/10.1101/2021.08.29.458125; this version posted August 31, 2021. The copyright holder for this preprint (which was not certified by peer review) is the author/funder, who has granted bioRxiv a license to display the preprint in perpetuity. It is made available under aCC-BY 4.0 International license.

795 Wagnon, J. L., & Meisler, M. H. (2015). Recurrent and Non-Recurrent Mutations of SCN8A in Epileptic
796 Encephalopathy. *Front Neurol, 6*, 104. doi:10.3389/fneur.2015.00104
797 Wengert, E. R., & Patel, M. K. (2021). The Role of the Persistent Sodium Current in Epilepsy. *Epilepsy*
798 *Curr, 21*(1), 40-47. doi:10.1177/1535759720973978
799 Wengert, E. R., Tronhjem, C. E., Wagnon, J. L., Johannesen, K. M., Petit, H., Krey, I., . . . Moller, R. S.
800 (2019). Biallelic inherited SCN8A variants, a rare cause of SCN8A-related developmental and
801 epileptic encephalopathy. *Epilepsia, 60*(11), 2277-2285. doi:10.1111/epi.16371
802 White, H. S., Johnson, M., Wolf, H. H., & Kupferberg, H. J. (1995). The early identification of
803 anticonvulsant activity: role of the maximal electroshock and subcutaneous pentylenetetrazol
804 seizure models. *Ital J Neurol Sci, 16*(1-2), 73-77. doi:10.1007/BF02229077
805 Yu, F. H., Mantegazza, M., Westenbroek, R. E., Robbins, C. A., Kalume, F., Burton, K. A., . . . Catterall, W.
806 A. (2006). Reduced sodium current in GABAergic interneurons in a mouse model of severe
807 myoclonic epilepsy in infancy. *Nat Neurosci, 9*(9), 1142-1149. doi:10.1038/nn1754
808 Zaman, T., Abou Tayoun, A., & Goldberg, E. M. (2019). A single-center SCN8A-related epilepsy cohort:
809 clinical, genetic, and physiologic characterization. *Ann Clin Transl Neurol, 6*(8), 1445-1455.
810 doi:10.1002/acn3.50839
811
812

bioRxiv preprint doi: https://doi.org/10.1101/2021.08.29.458125; this version posted August 31, 2021. The copyright holder for this preprint (which was not certified by peer review) is the author/funder, who has granted bioRxiv a license to display the preprint in perpetuity. It is made available under aCC-BY 4.0 International license.

Figure 1 Potency and isoform selectivity of NBI-921352 for human and mouse Na_V channels.

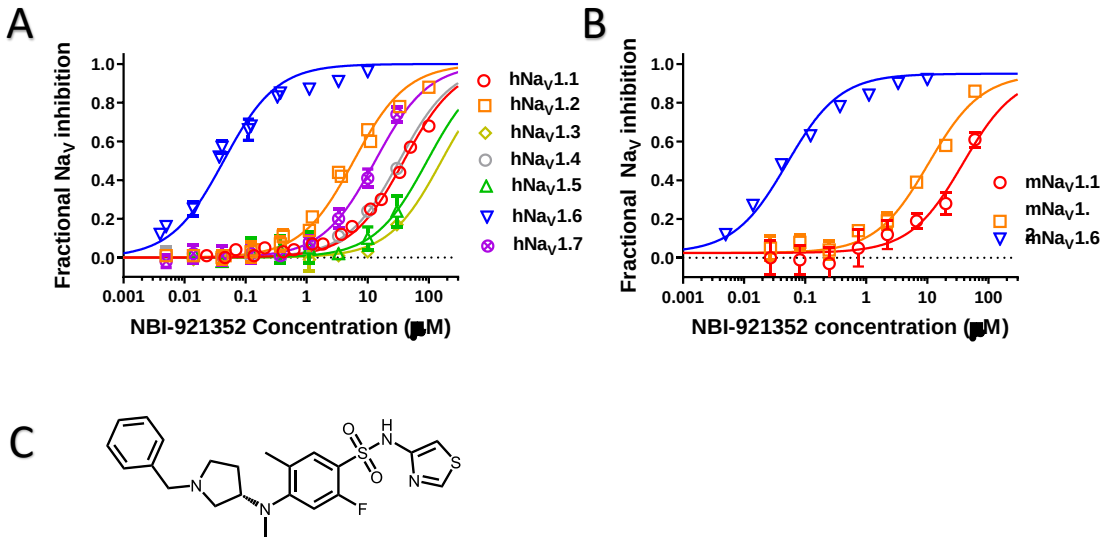

Concentration-response curves were generated by automated patch-clamp electrophysiology using the Sophion Qube. Concentration-response curves were generated for human (A) or mouse (B) Na_V channel isoforms heterologously expressed in HEK293 cells. The analysis included only those cells that met pre-specified acceptance criteria for seal quality, current amplitude, and series resistance. Normalized data from all cell recordings at a concentration were grouped together and plotted with GraphPad Prism 8. Details regarding the number of cells analyzed for each Na_V channel and concentration can be found in the source data sheet. Error bars indicating the standard error of the mean fraction were plotted for all points, but, in some cases, they were smaller than the data point symbols and, therefore, not visible. The chemical structure of NBI-921352 is shown (C).

bioRxiv preprint doi: https://doi.org/10.1101/2021.08.29.458125; this version posted August 31, 2021. The copyright holder for this preprint (which was not certified by peer review) is the author/funder, who has granted bioRxiv a license to display the preprint in perpetuity. It is made available under aCC-BY 4.0 International license.

826 **Table 1 Potency and isoform selectivity of NBI-921352 for human and mouse Na_V**

827 **channels.**

	$Na_V1.6$	$Na_V1.1$	$Na_V1.2$	$Na_V1.3$	$Na_V1.4$	$Na_V1.5$	$Na_V1.7$
Human IC_{50} (µM)	0.051	39	6.9	>30	>30	>30	14
Human Selectivity $hNa_V1.X$ / $hNa_V1.6$	1	756	134	>583	>583	>583	276
Mouse IC_{50} (µM)	0.058	41	11				
Mouse Selectivity $mNa_V1.X$ / $mNa_V1.6$	1	709	191				

828 IC_{50}s corresponding to the concentration-response curves in Figure 1 were calculated in GraphPad Prism
829 8 using the Hill equation described in the Materials and Methods. Note that IC_{50}s for the neuronal
830 sodium channels, Na_V 1.1, Na_V 1.2, and Na_V1.6, have been more accurately defined than those for non-
831 neuronal sodium channels.

832

bioRxiv preprint doi: https://doi.org/10.1101/2021.08.29.458125; this version posted August 31, 2021. The copyright holder for this preprint (which was not certified by peer review) is the author/funder, who has granted bioRxiv a license to display the preprint in perpetuity. It is made available under aCC-BY 4.0 International license.

Figure 2 Comparison of NBI-921352 potency on human wild-type $Na_V1.6$ and patient-identified variants of $Na_V1.6$.

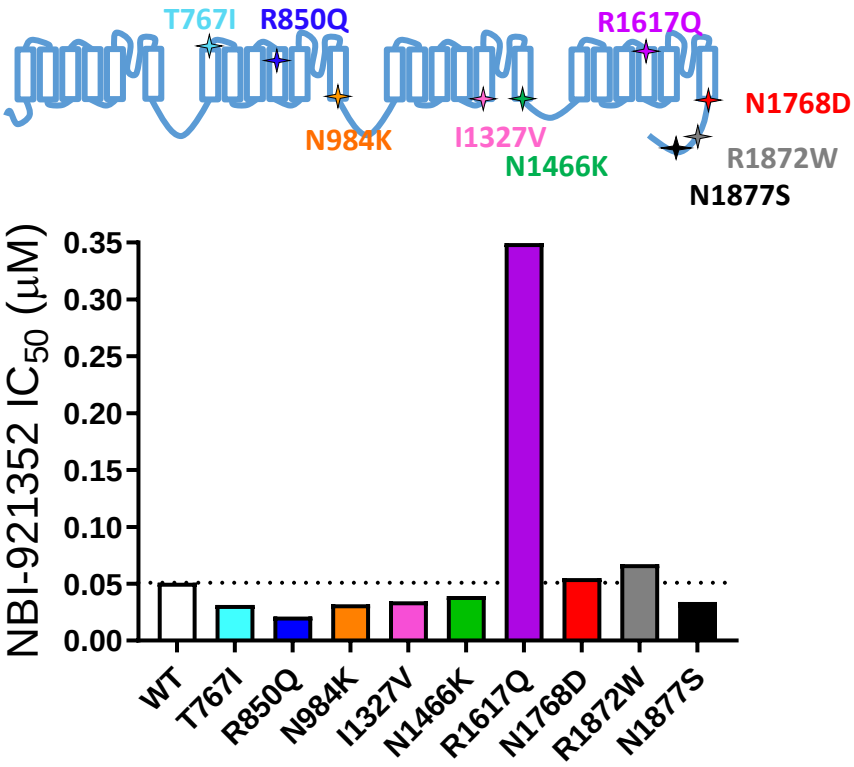

IC_{50}s were calculated in GraphPad Prism 8 using the Hill equation described in the Materials and Methods. All constructs were transiently transfected into Expi293F™ cells and evaluated by automated patch-clamp electrophysiology using the Sophion Qube. The voltage-clamp methods and data analysis were identical to those used for evaluation of the wild-type channels in Figure 1. Details regarding the number of cells analyzed for each Na_V channel and concentration can be found in the source data sheet. The dotted line indicates the IC_{50} for wild-type $Na_V1.6$ from Figure 1.

bioRxiv preprint doi: https://doi.org/10.1101/2021.08.29.458125; this version posted August 31, 2021. The copyright holder for this preprint (which was not certified by peer review) is the author/funder, who has granted bioRxiv a license to display the preprint in perpetuity. It is made available under aCC-BY 4.0 International license.

842

843 **Table 2 Comparison of NBI-921352 potency on human wild-type $Na_V1.6$ and patient-**

844 **identified gain-of-function variants of $Na_V1.6$.**

	WT	T767I	R850Q	N984K	I1327V	N1466K	R1617Q	N1768D	R1872W	N1877S
h$Na_V1.6$ IC_{50} (µM)	0.051	0.031	0.021	0.032	0.035	0.039	0.349	0.054	0.067	0.034
Fold change WT / Variant	-	0.6	0.4	0.6	0.7	0.8	6.8	1.1	1.3	0.7

845 IC_{50}s corresponding to Figure 2 are shown in the table and were calculated as indicated for Table 1.

846

bioRxiv preprint doi: https://doi.org/10.1101/2021.08.29.458125; this version posted August 31, 2021. The copyright holder for this preprint (which was not certified by peer review) is the author/funder, who has granted bioRxiv a license to display the preprint in perpetuity. It is made available under aCC-BY 4.0 International license.

847 **Figure 3 NBI-921352 is a state-dependent inhibitor of $Na_V1.6$ and preferentially inhibited**

848 **activated (open or inactivated) channels.**

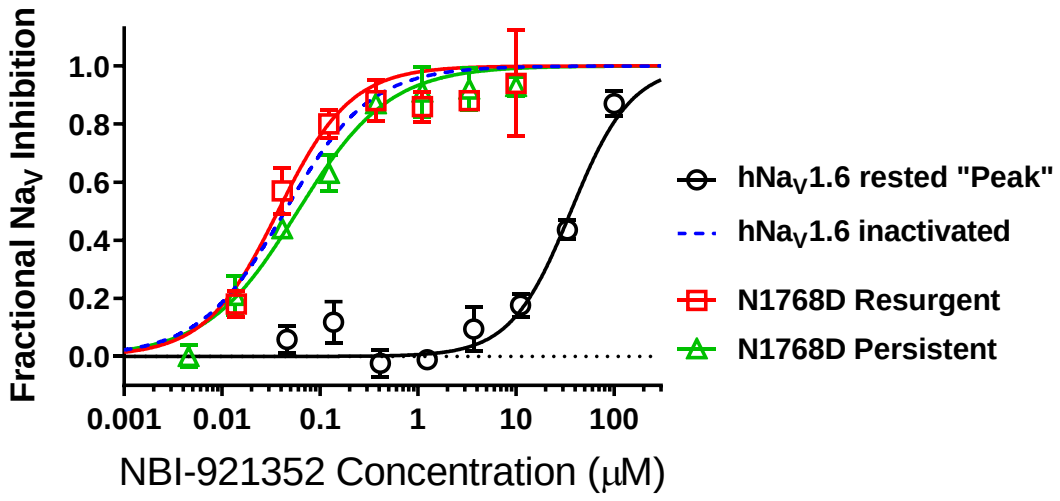

849

850 Concentration-response curves were generated for human WT and N1788D channel isoforms
851 heterologously expressed in HEK293 cells. The analysis included only those cells that met pre-specified
852 acceptance criteria for seal quality, current amplitude, and series resistance. Normalized data from all
853 cell recordings at a concentration were grouped together and plotted with GraphPad Prism 8. Details
854 regarding the number of cells analyzed for each Na_V channel isoform and concentration can be found in
855 the source data sheet. Error bars indicating the standard error of the mean fraction were plotted for all
856 points. The blue dotted line indicates the concentration-response curve for wild-type $Na_V1.6$ from
857 Figure 1. When $Na_V1.6$ channels were equilibrated with NBI-921352 at voltages that allow full
858 equilibration with inactivated states (-45 mV), the compound provided potent inhibition, as seen in
859 Figure 1. Measuring persistent or resurgent sodium current after equilibration of cells with NBI-921352
860 resulted in similar potency (see Materials and Methods and text). Forcing channels to the rested, closed
861 state by hyperpolarizing to -120 mV resulted in very weak inhibition. Current evoked from very negative
862 potentials is sometimes referred to as “peak current”.

bioRxiv preprint doi: https://doi.org/10.1101/2021.08.29.458125; this version posted August 31, 2021. The copyright holder for this preprint (which was not certified by peer review) is the author/funder, who has granted bioRxiv a license to display the preprint in perpetuity. It is made available under aCC-BY 4.0 International license.

863 **Figure 4 NBI-921352 inhibits firing in pyramidal neurons but spares fast-spiking**

864 **interneurons.**

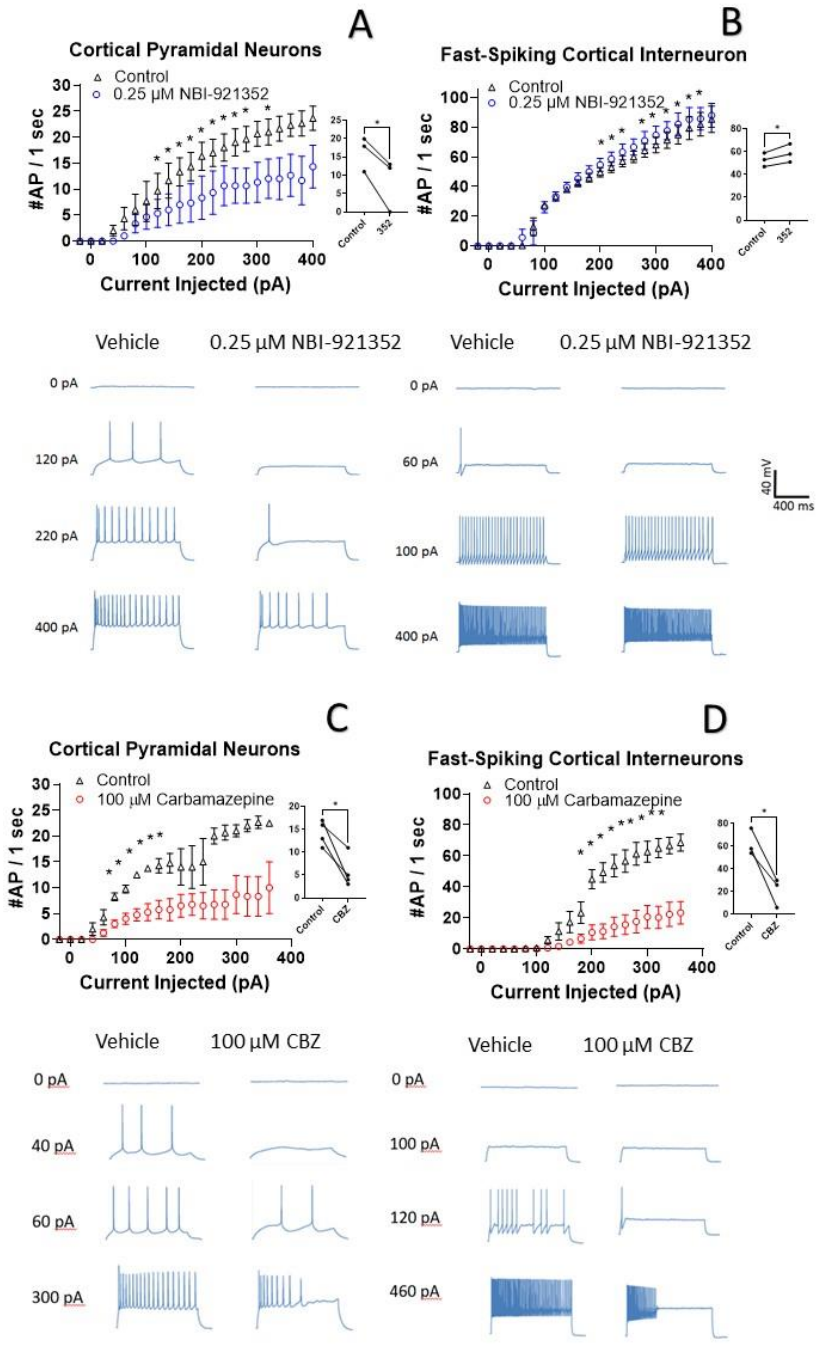

865

bioRxiv preprint doi: https://doi.org/10.1101/2021.08.29.458125; this version posted August 31, 2021. The copyright holder for this preprint (which was not certified by peer review) is the author/funder, who has granted bioRxiv a license to display the preprint in perpetuity. It is made available under aCC-BY 4.0 International license.

866 Current input versus action-potential output evaluations in wild-type mouse brain slices treated with
867 vehicle or 0.25 µM NBI-921352 (A & B), or 100 µM carbamazepine (C & D) was plotted. In cortical
868 pyramidal neurons, both NBI-921352 (A) and carbamazepine (C) reduced AP spiking. In fast-spiking
869 cortical interneurons, NBI-921352 increased firing frequency slightly (B), while carbamazepine markedly
870 reduced firing (D). The main upper panels compare average AP count of 3-4 neurons in each condition
871 +/- the standard error of the mean. The inserts in the upper panels show the results for each tested
872 neuron at approximately 3X the cell rheobase. *Indicates a $p<0.05$ relative to the control condition
873 using a paired, two-way, student's t-test. The lower panels show recordings for individual representative
874 neurons for each condition. No inhibitors of synaptic inputs were used for these experiments.

875

bioRxiv preprint doi: https://doi.org/10.1101/2021.08.29.458125; this version posted August 31, 2021. The copyright holder for this preprint (which was not certified by peer review) is the author/funder, who has granted bioRxiv a license to display the preprint in perpetuity. It is made available under aCC-BY 4.0 International license.

Figure 5 NBI-921352 inhibited electrically induced seizures in rodents.

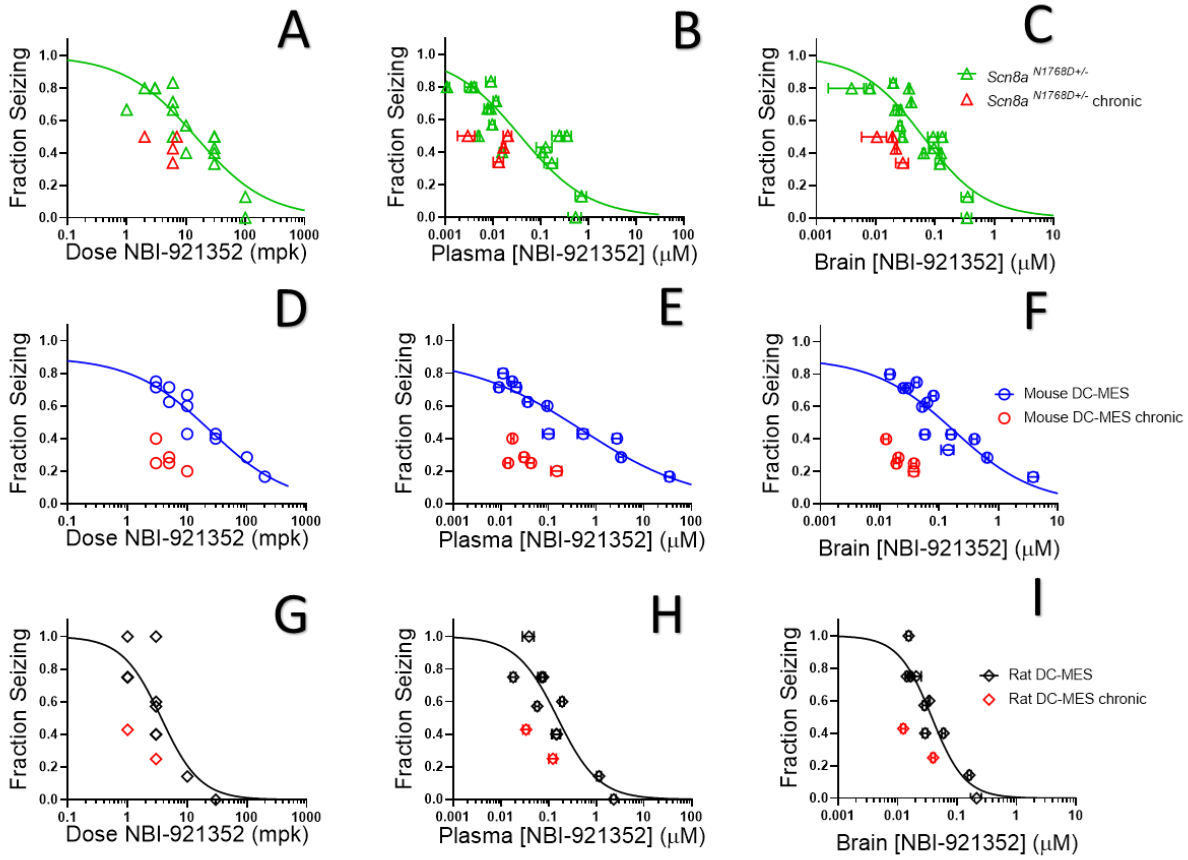

Dose versus efficacy, plasma concentration versus efficacy, and brain concentration versus efficacy relations are shown for *Scn8a*$^{N1768D+/-}$ mice in the modified 6Hz psychomotor seizure assay in A, B, and C, respectively (green open triangles). Dose versus efficacy, plasma concentration versus efficacy, and brain concentration versus efficacy relations are shown for wild-type mice in the DC-MES assay in D, E, and F, respectively (blue open circles). Dose versus efficacy, plasma concentration versus efficacy, and brain concentration versus efficacy relations are shown for wild-type rats in the DC-MES assay in G, H, and I, respectively (black open diamonds). Each point represents the fraction of animals exhibiting a GTC with hindlimb extension after stimulus from a dosing group of 4-8 animals (See source data sheet for all additional information). Horizontal error bars show the standard error of the mean plasma (B, E, H) or

bioRxiv preprint doi: https://doi.org/10.1101/2021.08.29.458125; this version posted August 31, 2021. The copyright holder for this preprint (which was not certified by peer review) is the author/funder, who has granted bioRxiv a license to display the preprint in perpetuity. It is made available under aCC-BY 4.0 International license.

887 brain (C, F, I) concentrations measured from the animals in that dosing group immediately after assay.

888 Where error bars are not visible, they are smaller than the symbols. No error bars are shown for the dose

889 levels (A, D, G), since those were dictated by the experimenter.

890

bioRxiv preprint doi: https://doi.org/10.1101/2021.08.29.458125; this version posted August 31, 2021. The copyright holder for this preprint (which was not certified by peer review) is the author/funder, who has granted bioRxiv a license to display the preprint in perpetuity. It is made available under aCC-BY 4.0 International license.

891 **Figure 6 NBI-921352 is more potent than 3 commonly prescribed Na_V inhibitor ASMs.**

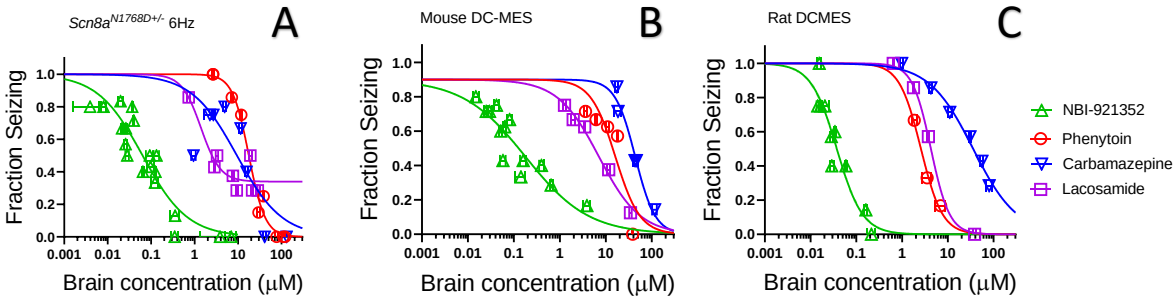

892

893 Brain concentration versus fraction of animals exhibiting is plotted for NBI-921352 versus that for
894 phenytoin, carbamazepine, and lacosamide in the *Scn8a*$^{N1768D+/-}$ modified 6Hz model (A), the wild-type
895 mouse DC-MES model (B), and the wild-type rat DC-MES model (C). Data from animals at a given dose
896 were grouped together and plotted with GraphPad Prism 8. Details regarding the number of animals
897 analyzed per model and per dose group can be found in the source data sheet. Error bars indicating the
898 standard error of the mean concentration were plotted for all points on the concentration-response
899 curves.

900

bioRxiv preprint doi: https://doi.org/10.1101/2021.08.29.458125; this version posted August 31, 2021. The copyright holder for this preprint (which was not certified by peer review) is the author/funder, who has granted bioRxiv a license to display the preprint in perpetuity. It is made available under aCC-BY 4.0 International license.

Figure 7 Rat efficacy compared to acute tolerability for NBI-921352 relative to Na_V inhibitor ASMs.

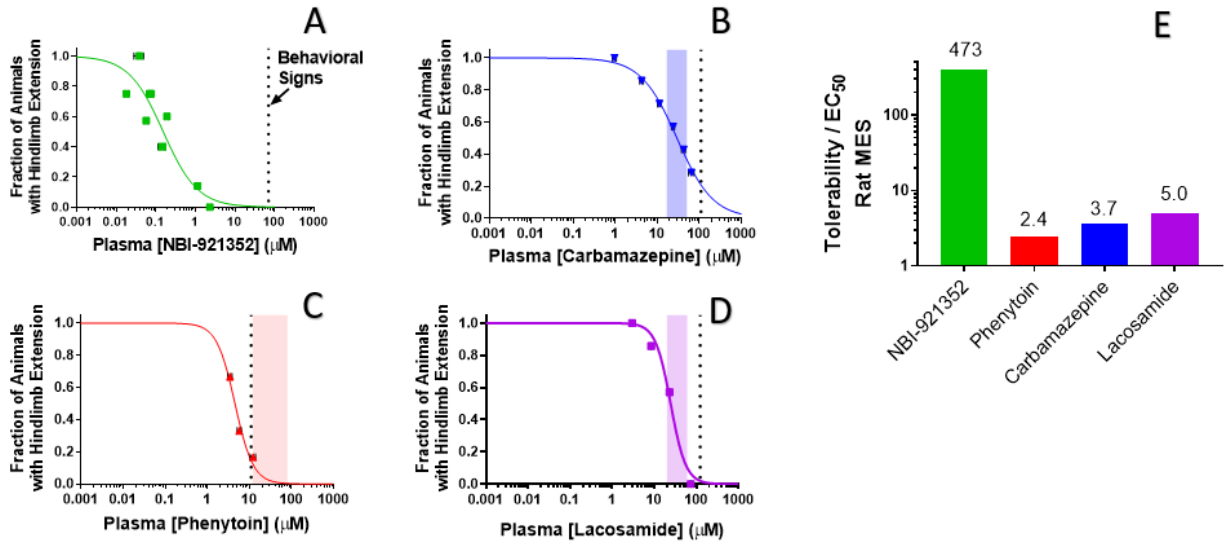

Plasma concentration versus efficacy data is shown for the rat DC-MES assay for NBI-921352 (A), carbamazepine (B), phenytoin (C), and lacosamide (D). The vertical dotted lines indicate the lowest plasma concentration at which a rat was observed to exhibit atypical behavioral signs indicative of an adverse reaction to drug in the assay format. Animals exhibiting such signs were excluded from efficacy evaluation. The shaded bars in B, C, and D indicate the approximate human plasma concentrations observed in clinical practice. Data from animals at a given dose were grouped together and plotted with GraphPad Prism 8. Details regarding the number of animals analyzed per model and per dose group can be found in the source data sheet. Error bars indicating the standard error of the mean concentration were plotted for all points on the concentration-response curves. Panel E shows the ratio of the (rat plasma EC_{50} / the plasma concentration where behavioral signs were noted for each compound).